

4th European sCO<sub>2</sub> Conference 2021, March 23-24

## NUMERICAL ANALYSIS OF A CENTRIFUGAL COMPRESSOR OPERATING WITH SUPERCRITICAL CO<sub>2</sub>

Renan Emre Karaefe<sup>1</sup>, Pascal Post<sup>1</sup>, Marwick Sembritzky<sup>1</sup>, Andreas Schramm<sup>1</sup>, Matthias Kunick<sup>2</sup>, Uwe Gampe<sup>3</sup>, Francesca di Mare<sup>1</sup>

<sup>1</sup>Ruhr Universität Bochum  
Faculty of Mechanical Engineering  
Chair of Thermal Turbomachines and Aeroengines  
44801 Bochum, Germany

<sup>2</sup>Zittau/Goerlitz University of Applied Sciences  
Faculty of Mechanical Engineering  
Dept. of Energy Systems Technology  
02763 Zittau, Germany

<sup>3</sup>Technische Universität Dresden  
Faculty of Mechanical Science and Engineering  
Chair of Thermal Power Machinery and Plants  
01062 Dresden, Germany



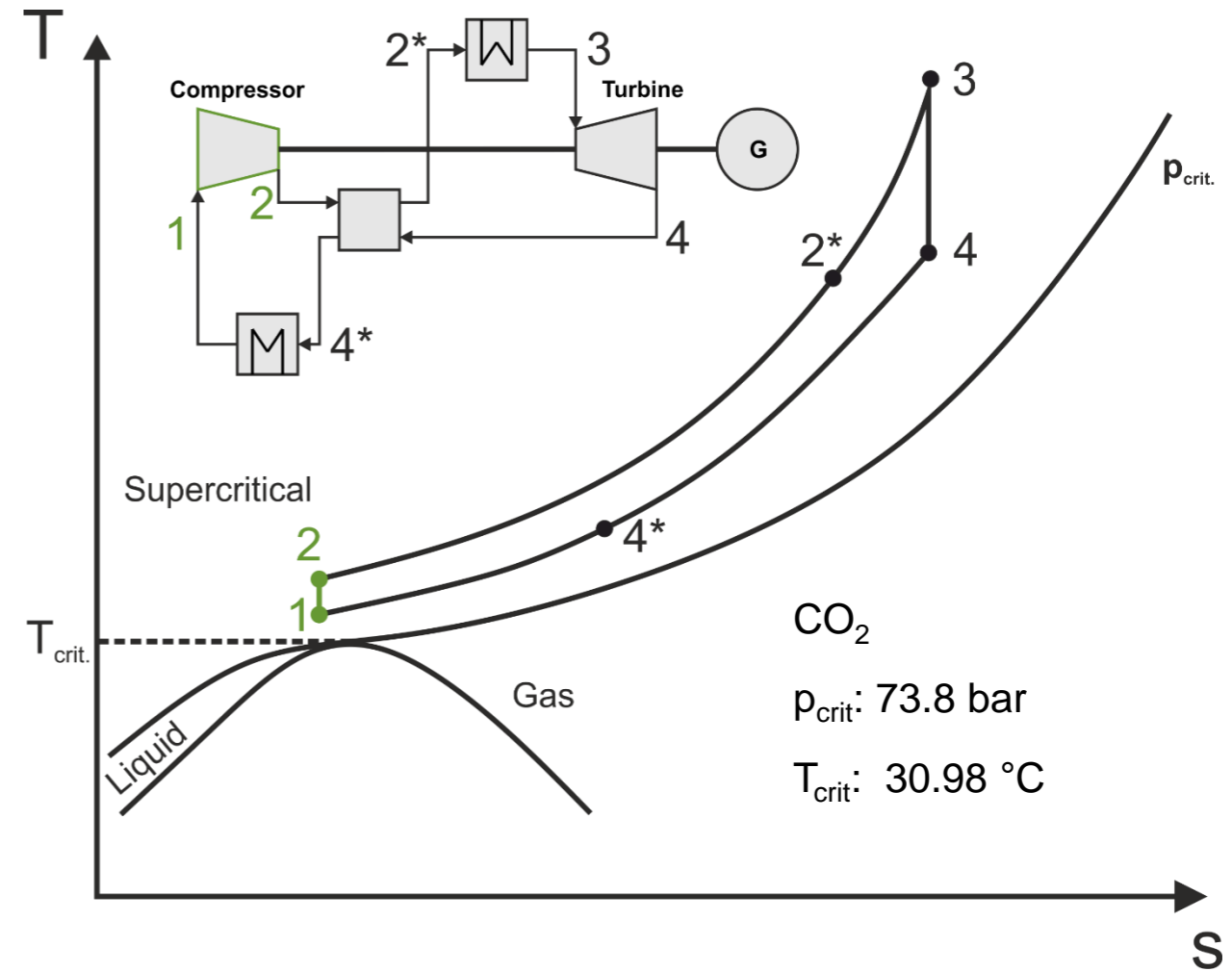
**RUHR-UNIVERSITÄT BOCHUM**

**CHAIR OF THERMAL TURBOMACHINES AND AEROENGINES**

## sCO<sub>2</sub>-Power Systems

### Characteristics

- Low compression work
- Small scale of turbomachinery
- Comparatively high efficiency in the mild turbine inlet temperature range (450 - 600°C)



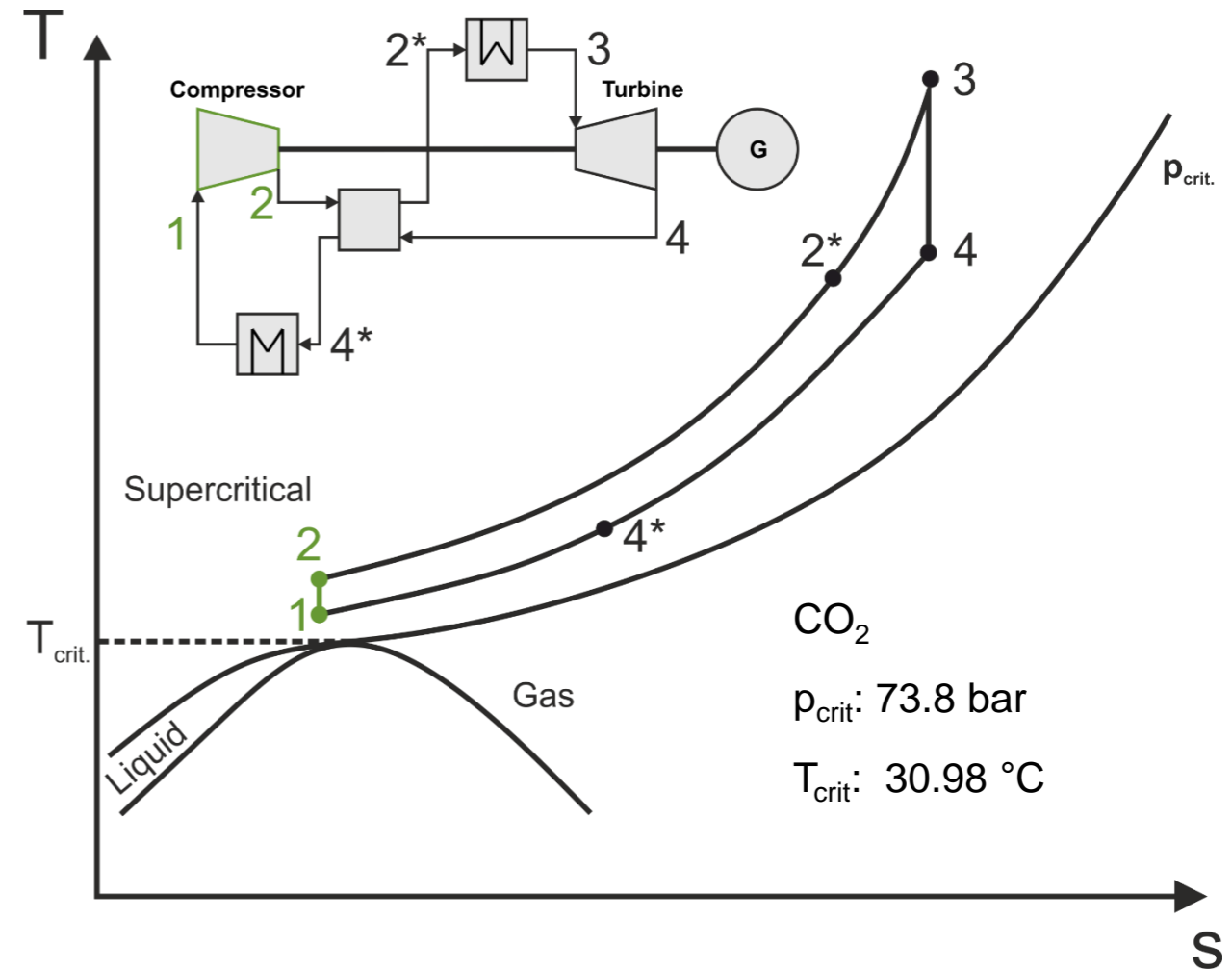
## sCO<sub>2</sub>-Power Systems

### Characteristics

- Low compression work
- Small scale of turbomachinery
- Comparatively high efficiency in the mild turbine inlet temperature range (450 - 600°C)

### Application Areas

- Topping cycle for fossil fueled power plants
- Bottoming cycle for gas combined cycles
- Renewable energy
- Exhaust/waste heat recovery
- Nuclear energy



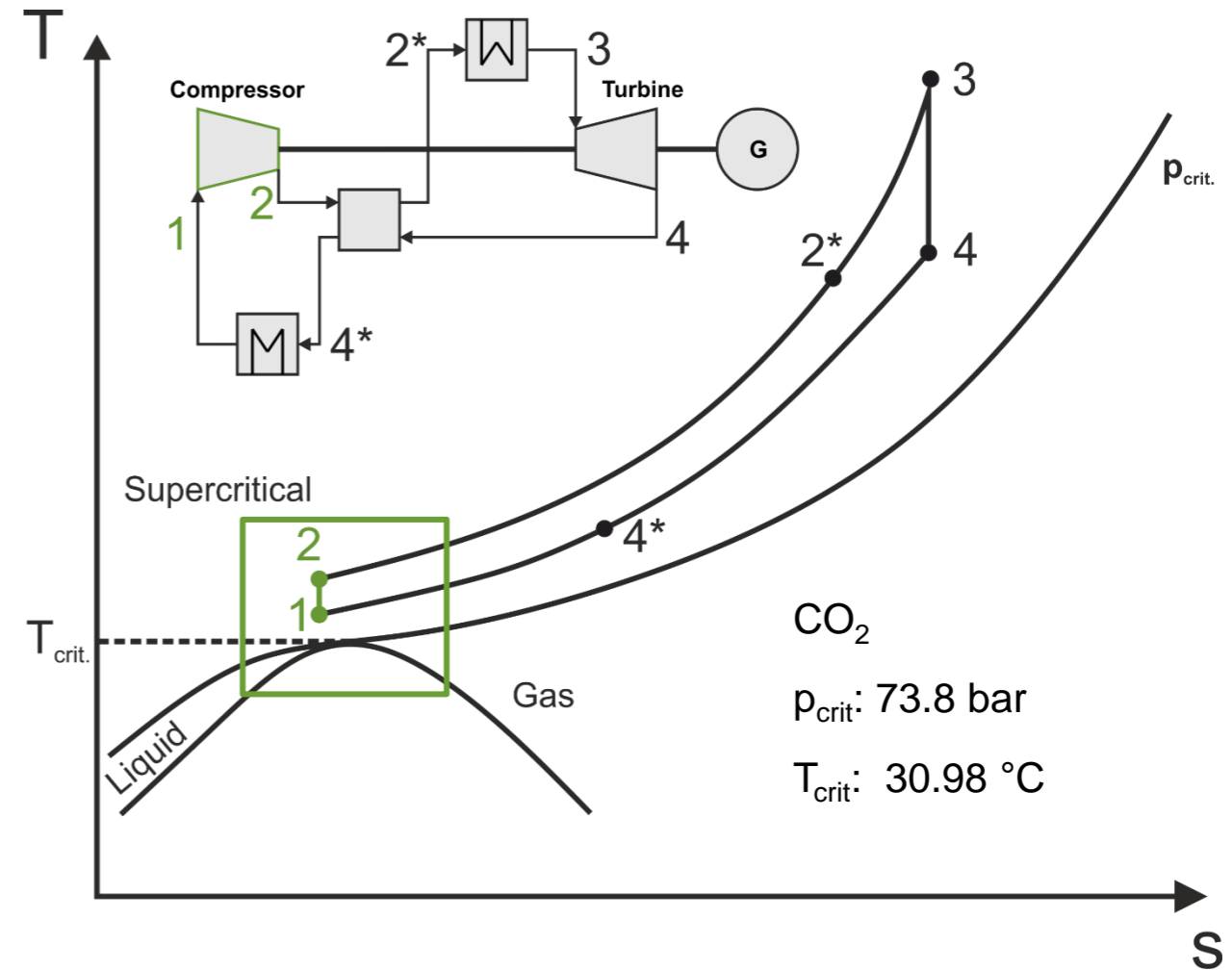
## sCO<sub>2</sub>-Power Systems

### Characteristics

- Low compression work
- Small scale of turbomachinery
- Comparatively high efficiency in the mild turbine inlet temperature range (450 - 600°C)

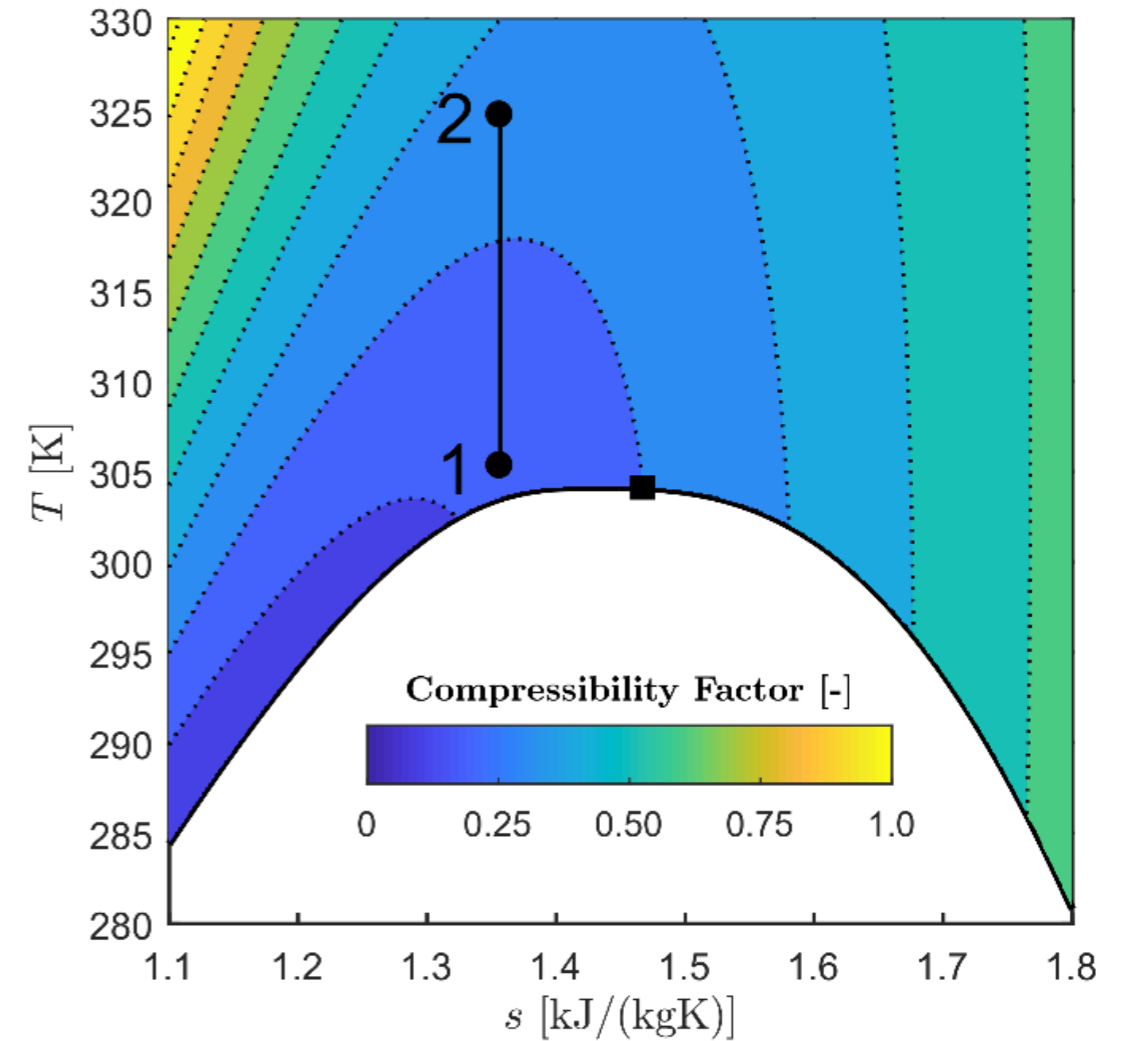
### Application Areas

- Topping cycle for fossil fueled power plants
- Bottoming cycle for gas combined cycles
- Renewable energy
- Exhaust/waste heat recovery
- Nuclear energy



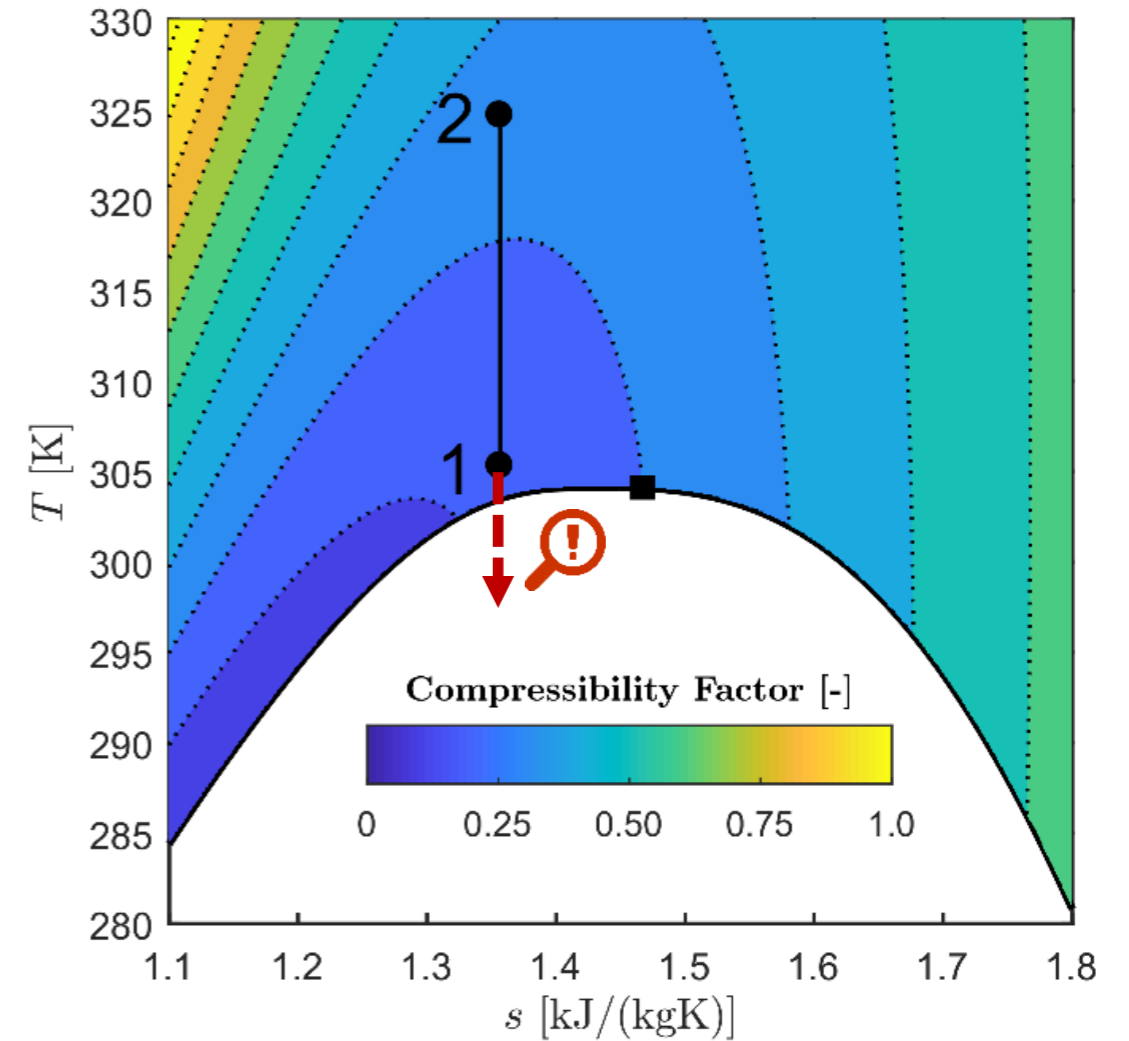
## Challenges for Aerothermal Compressor Design and Analysis

- Non-ideal thermophysical properties



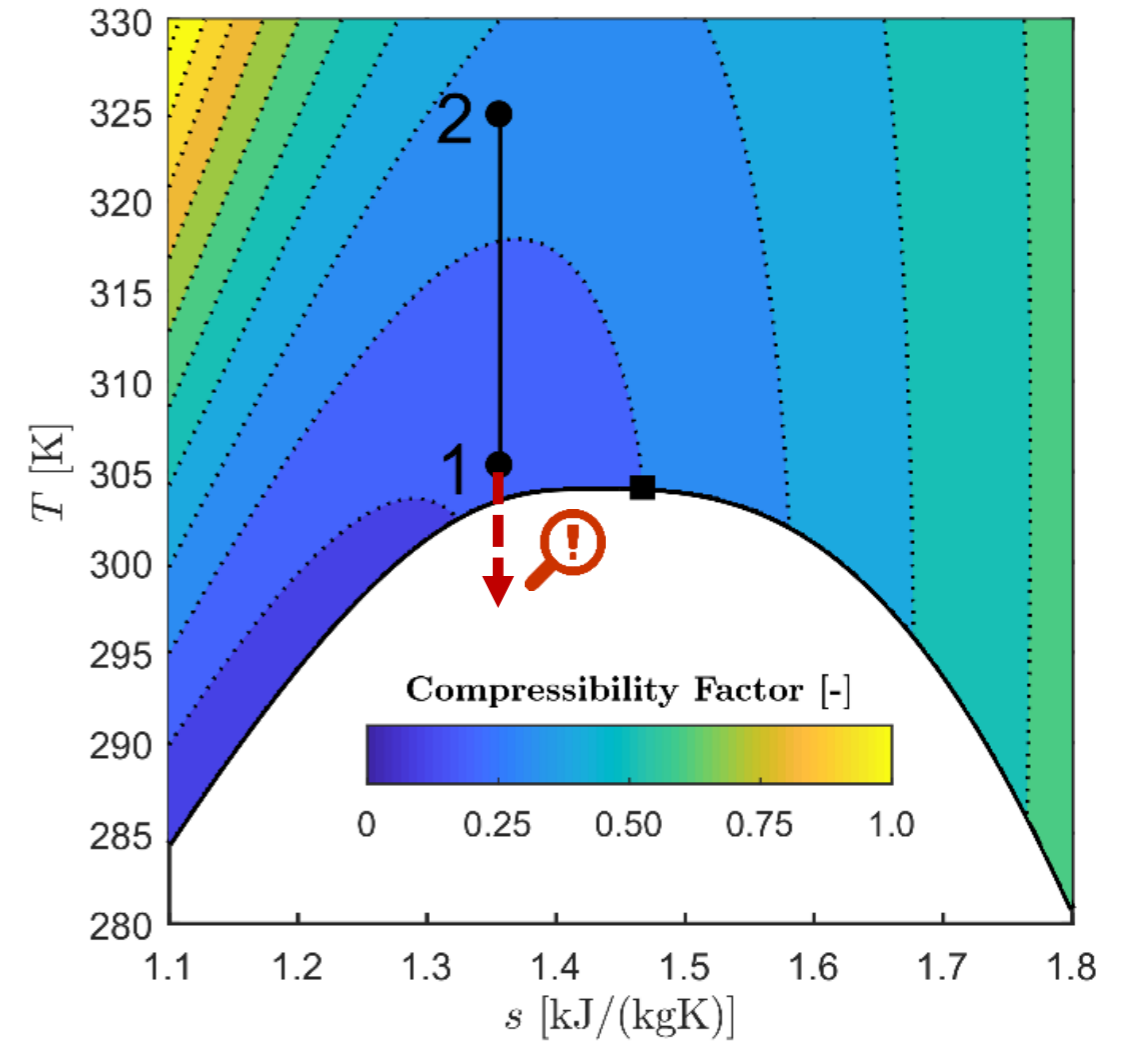
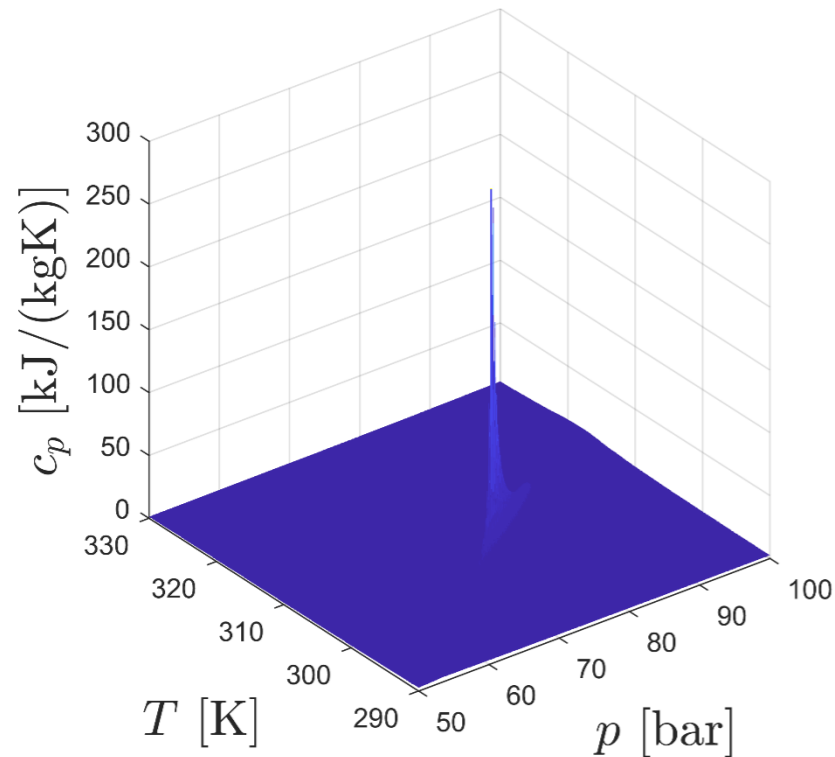
## Challenges for Aerothermal Compressor Design and Analysis

- Non-ideal thermophysical properties
- Possibility of two-phase flows (locally)



## Challenges for Aerothermal Compressor Design and Analysis

- Non-ideal thermophysical properties
- Possibility of two-phase flows (locally)
- Rapidly changing fluid properties in the vicinity of the critical point



## Scope of work

- Extension of the in-house CFD solver to account for thermophysical properties of  $s\text{CO}_2$  with high degree of accuracy and numerical stability



## Scope of work

- Extension of the in-house CFD solver to account for thermophysical properties of  $s\text{CO}_2$  with high degree of accuracy and numerical stability
  - Span-Wagner multiparameter EOS [1] is too computationally expensive

## Scope of work

- Extension of the in-house CFD solver to account for thermophysical properties of  $s\text{CO}_2$  with high degree of accuracy and numerical stability
  - Span-Wagner multiparameter EOS [1] is too computationally expensive
  - Integration via Spline Based Table Lookup Method [2, 3]

## Scope of work

- Extension of the in-house CFD solver to account for thermophysical properties of sCO<sub>2</sub> with high degree of accuracy and numerical stability
  - Span-Wagner multiparameter EOS [1] is too computationally expensive
  - Integration via Spline Based Table Lookup Method [2, 3]
- Validation of the CFD framework for sCO<sub>2</sub> compressor performance and flow field assessments

## Scope of work

- Extension of the in-house CFD solver to account for thermophysical properties of sCO<sub>2</sub> with high degree of accuracy and numerical stability
  - Span-Wagner multiparameter EOS [1] is too computationally expensive
  - Integration via Spline Based Table Lookup Method [2, 3]
- Validation of the CFD framework for sCO<sub>2</sub> compressor performance and flow field assessments
  - Lack of fully documented experimental test cases

## Scope of work

- Extension of the in-house CFD solver to account for thermophysical properties of sCO<sub>2</sub> with high degree of accuracy and numerical stability
  - Span-Wagner multiparameter EOS [1] is too computationally expensive
  - Integration via Spline Based Table Lookup Method [2, 3]
- Validation of the CFD framework for sCO<sub>2</sub> compressor performance and flow field assessments
  - Lack of fully documented experimental test cases
  - Investigation of a geometry based on the main dimensions of the SNL main compressor

## Scope of work

- Extension of the in-house CFD solver to account for thermophysical properties of sCO<sub>2</sub> with high degree of accuracy and numerical stability
  - Span-Wagner multiparameter EOS [1] is too computationally expensive
  - Integration via Spline Based Table Lookup Method [2, 3]
- Validation of the CFD framework for sCO<sub>2</sub> compressor performance and flow field assessments
  - Lack of fully documented experimental test cases
  - Investigation of a geometry based on the main dimensions of the SNL main compressor
- Development and validation of a sCO<sub>2</sub> compressor performance meanline analysis tool

## Scope of work

- Extension of the in-house CFD solver to account for thermophysical properties of sCO<sub>2</sub> with high degree of accuracy and numerical stability
  - Span-Wagner multiparameter EOS [1] is too computationally expensive
  - Integration via Spline Based Table Lookup Method [2, 3]
- Validation of the CFD framework for sCO<sub>2</sub> compressor performance and flow field assessments
  - Lack of fully documented experimental test cases
  - Investigation of a geometry based on the main dimensions of the SNL main compressor
- Development and validation of a sCO<sub>2</sub> compressor performance meanline analysis tool
  - Further reference for performance assessments

## Scope of work

- Extension of the in-house CFD solver to account for thermophysical properties of sCO<sub>2</sub> with high degree of accuracy and numerical stability
  - Span-Wagner multiparameter EOS [1] is too computationally expensive
  - Integration via Spline Based Table Lookup Method [2, 3]
- Validation of the CFD framework for sCO<sub>2</sub> compressor performance and flow field assessments
  - Lack of fully documented experimental test cases
  - Investigation of a geometry based on the main dimensions of the SNL main compressor
- Development and validation of a sCO<sub>2</sub> compressor performance meanline analysis tool
  - Further reference for performance assessments
  - Breakdown of individual loss contributions

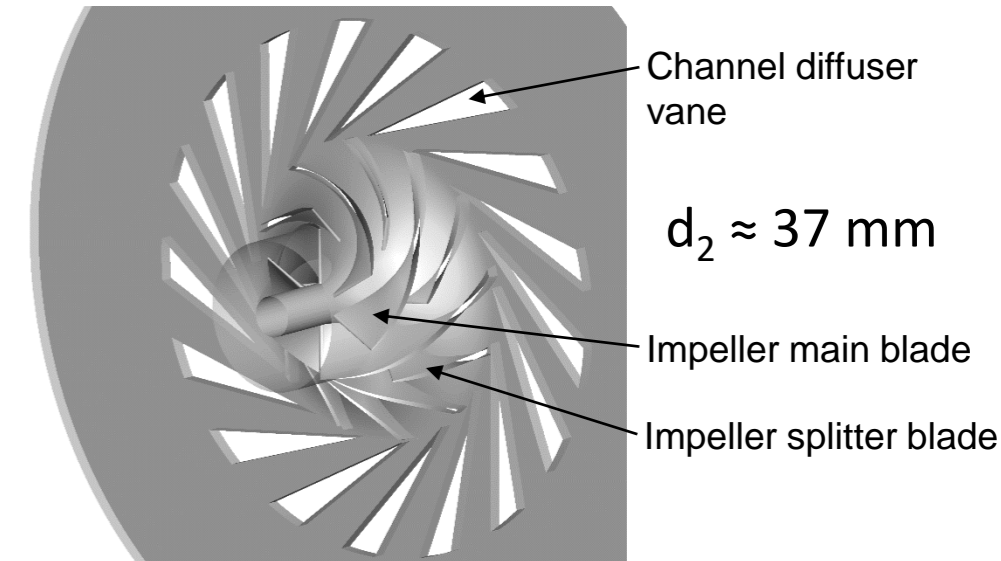


- 1 Motivation
- 2 Test Case Description
- 3 Methodology
- 4 Results
- 5 Conclusion and Consecutive Work

## SNL Compressor

- Candidate geometry based on main dimensions of the SNL compression test-loop main compressor
  - Backward swept impeller ( $50^\circ$ ), 6 main blades + 6 splitter blades
  - Channel diffuser, 17 vanes
  - Design specifications:  
 $50 \text{ kWe} \mid 75 \text{ krpm} \mid 3.54 \text{ kg}\cdot\text{s}^{-1} \mid \eta_{ts} \approx 66\% \mid \pi = 1,8$   
 $T_{0,in}/T_c \approx 1.004 \mid p_{0,in}/p_c \approx 1.04 \mid \rho_{0,in} \approx 576 \text{ kg}\cdot\text{m}^{-3}$

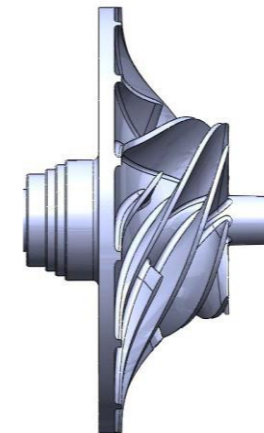
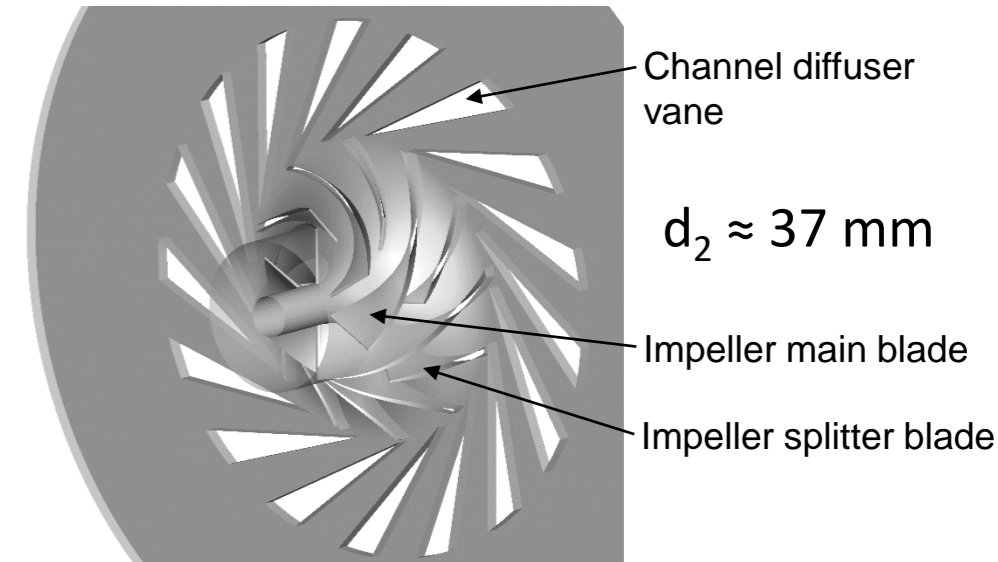
CAD model of the investigated stage geometry



## SNL Compressor

- Candidate geometry based on main dimensions of the SNL compression test-loop main compressor
  - Backward swept impeller ( $50^\circ$ ), 6 main blades + 6 splitter blades
  - Channel diffuser, 17 vanes
  - Design specifications:  
 $50 \text{ kWe}$  |  $75 \text{ krpm}$  |  $3.54 \text{ kg}\cdot\text{s}^{-1}$  |  $\eta_{ts} \approx 66\%$  |  $\pi = 1,8$   
 $T_{0,in}/T_c \approx 1.004$  |  $p_{0,in}/p_c \approx 1.04$  |  $\rho_{0,in} \approx 576 \text{ kg}\cdot\text{m}^{-3}$
- Restrictions
  - Main dimensions reported partially
  - No blade coordinates accessible  
→ Correct reconstruction of blade angle and thickness distribution is not possible

CAD model of the investigated stage geometry

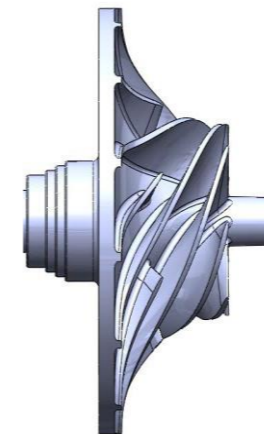
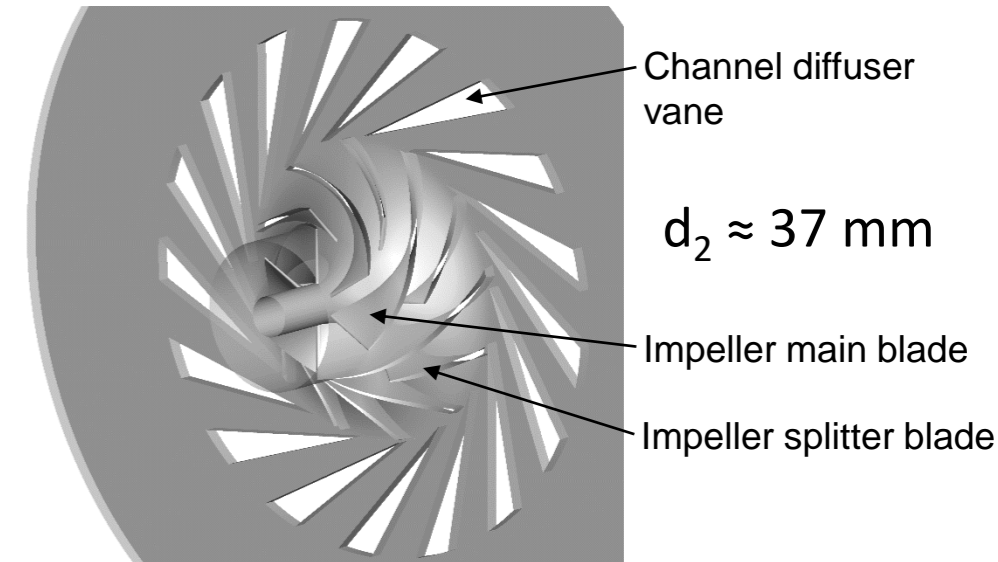


Part drawing and photograph of the SNL main compressor [4]

## SNL Compressor

- Candidate geometry based on main dimensions of the SNL compression test-loop main compressor
  - Backward swept impeller ( $50^\circ$ ), 6 main blades + 6 splitter blades
  - Channel diffuser, 17 vanes
  - Design specifications:  
 $50 \text{ kWe}$  |  $75 \text{ krpm}$  |  $3.54 \text{ kg}\cdot\text{s}^{-1}$  |  $\eta_{ts} \approx 66\%$  |  $\pi = 1,8$   
 $T_{0,in}/T_c \approx 1.004$  |  $p_{0,in}/p_c \approx 1.04$  |  $\rho_{0,in} \approx 576 \text{ kg}\cdot\text{m}^{-3}$
- Restrictions
  - Main dimensions reported partially
  - No blade coordinates accessible  
→ Correct reconstruction of blade angle and thickness distribution is not possible
- Simplifications
  - No tip clearance modeled

CAD model of the investigated stage geometry



Part drawing and photograph of the SNL main compressor [4]

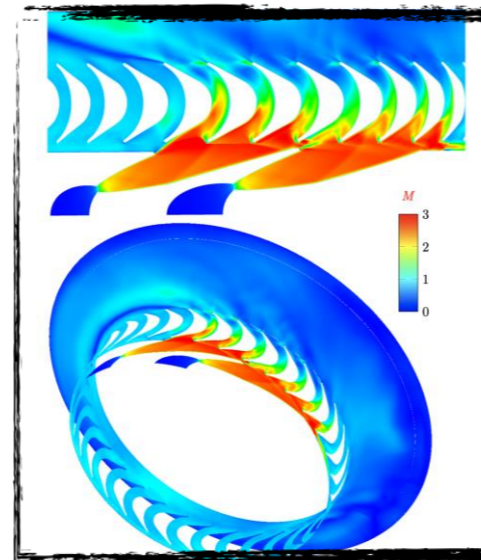
## CFD Solver

- In-house density based solver
- Hybrid parallelization
- Complex thermodynamic applications

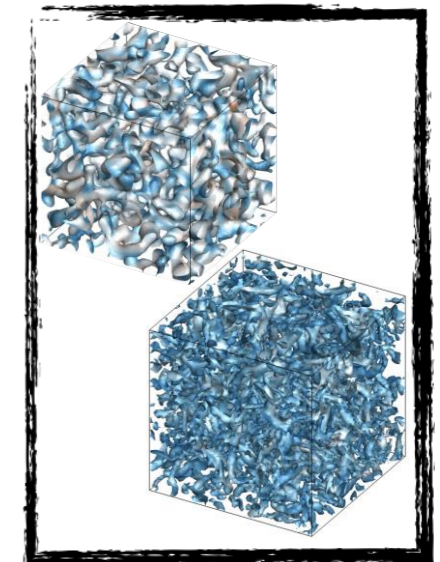
CONDENSING WET STEAM (LES) [6]



ORC [5]



DNS/LES



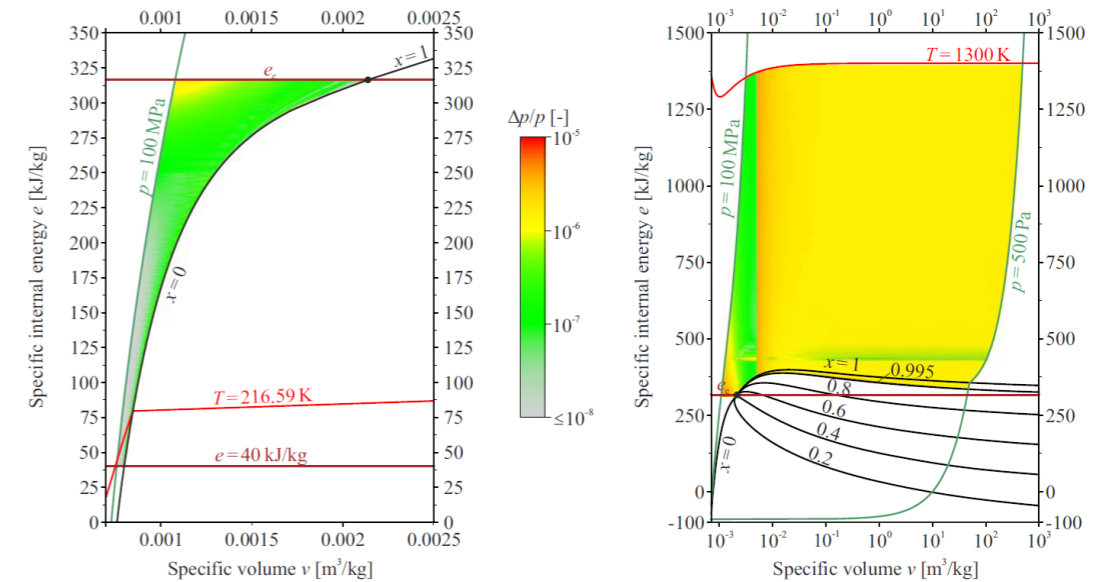
## Real Gas Property Tabulation

- Spline Based Table Lookup Method (SBTL) [2, 3]
  - Biquadratic polynomial spline interpolation
  - Continuous first derivatives
  - Numerically fast and consistent backward functions
  - Constructed on piecewise equidistant nodes
- Tabulated data is based on the Span-Wagner reference EOS [1] and correlations for viscosity and thermal conductivity [7, 8]
- Permissible deviations are within uncertainties of the underlying equations/correlations

[2] M. Kunick. "Fast Calculation of Thermophysical Properties in Extensive Process Simulations with the Spline-Based Table Look-Up Method (SBTL)". Fortschrittberichte VDI, Nr. 618, Reihe 6, Energietechnik, 2018.

[3] M. Kunick et al. "CFD Analysis of Steam Turbines With the IAPWS Standard on the Spline-Based Table Look-Up Method (SBTL) for The Fast Calculation of Real Fluid Properties". Proceedings of ASME Turbo Expo 2015, ASME Paper No. GT2015-43984, 2015.

### Permissible deviations of spline-functions (CO<sub>2</sub> application)

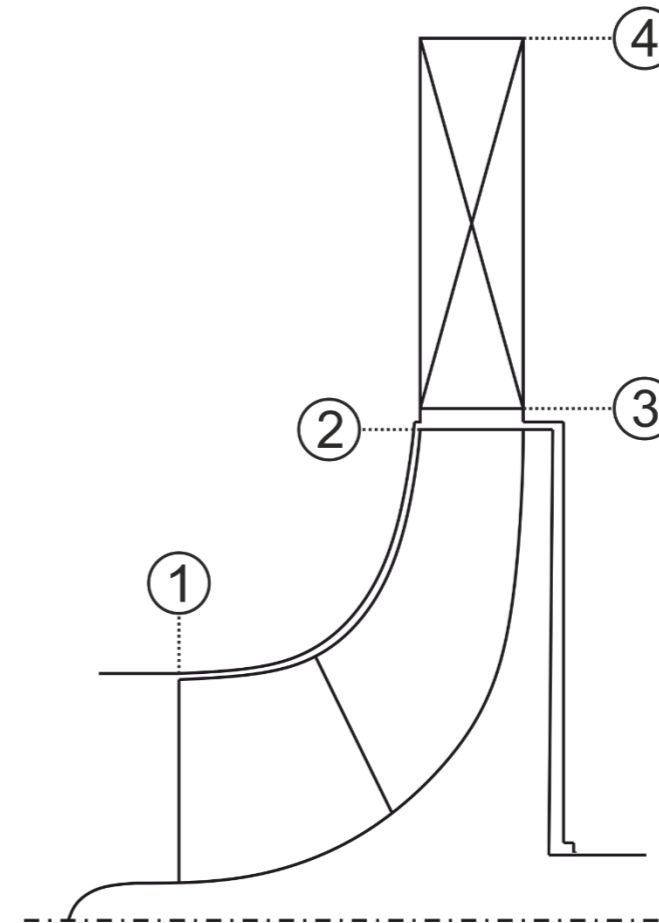


[9]

SBTL function	liquid region	gas region
$p(v, e)$	$p \leq 2.5 \text{ Mpa}$ $ \Delta p/p  < 0.001\%$ $p > 2.5 \text{ Mpa}$ $ \Delta p  < 0.5 \text{ kPa}$	$ \Delta p/p  < 0.001\%$
$T(v, e)$	$ \Delta T  < 1 \text{ mK}$	$ \Delta T  < 1 \text{ mK}$
$s(v, e)$	$ \Delta s  < 10^{-6} \text{ kJ}/(\text{kg K})$	$ \Delta s  < 10^{-6} \text{ kJ}/(\text{kg K})$
$w(v, e)$	$ \Delta w/w  < 0.001\%$	$ \Delta w/w  < 0.001\%$
$\eta(v, e)$	$ \Delta \eta/\eta  < 0.001\%$	$ \Delta \eta/\eta  < 0.001\%$
$\lambda(v, e)$	$ \Delta \lambda/\lambda  < 0.001\%$	$ \Delta \lambda/\lambda  < 0.001\%$

## Meanline Analysis Method

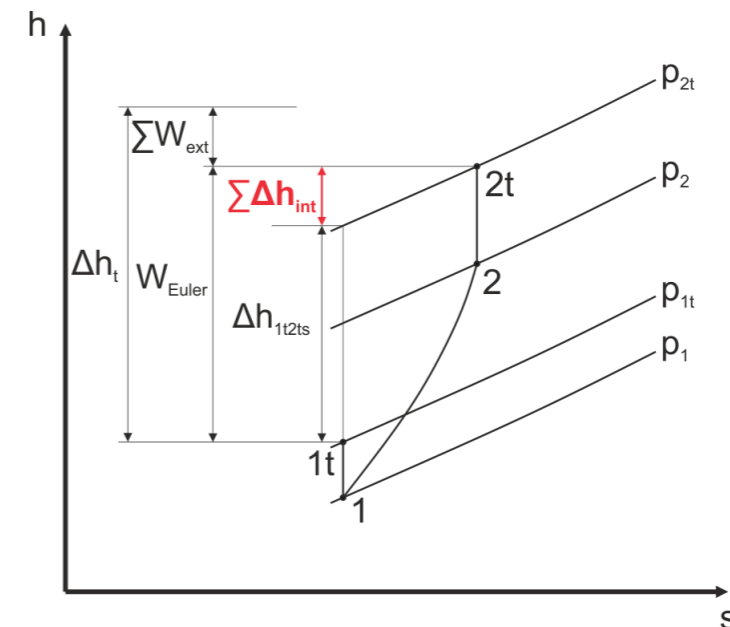
- Single-zone modeling approach
- Implemented in PYTHON with direct calls to the CoolProp [10] property library



## Meanline Analysis Method

- Single-zone modeling approach
- Implemented in PYTHON with direct calls to the CoolProp [10] property library
- Applied loss model set is based on an optimised and validated set of internal and external loss for conventional centrifugal compressors (Oh et al. [11])

Loss mechanism	Loss model	Reference
<b>Impeller</b>		
Incidence	$\Delta h_{inc} = \sigma \cdot \frac{(w_{1\theta} - w_{1\theta,bl})^2}{2}$	Conrad et al. [12]
Blade loading	$\Delta h_{bl} = 0.05 \cdot D_f^2 \cdot u_2^2$	Coppage et al. [13]
Skin friction	$\Delta h_{sf} = 2c_f \frac{L_{fl}}{d_{hb}} \bar{w}^2$	Jansen [14]
Clearance	$\Delta h_{cl} = u_2^2 \cdot 0.6 \frac{\delta_{cl}}{b_2} \frac{c_{2\theta}}{u_2} \times \sqrt{\frac{4\pi}{b_2 Z_{bl}} \left[ \frac{r_{1t}^2 - r_{1h}^2}{(r_2 - r_{1t})(1 - \rho_2/\rho_1)} \right] \frac{c_{2\theta}}{u_2} \frac{c_{1m}}{u_2}}$	Jansen [14]
Mixing	$\Delta h_{mix} = \frac{c_2^2}{2[1 + (c_{2\theta}/c_{2m})^2]} \cdot \left[ \frac{1 - \varepsilon - B}{1 - \varepsilon} \right]^2$	Johnston & Dean [15]

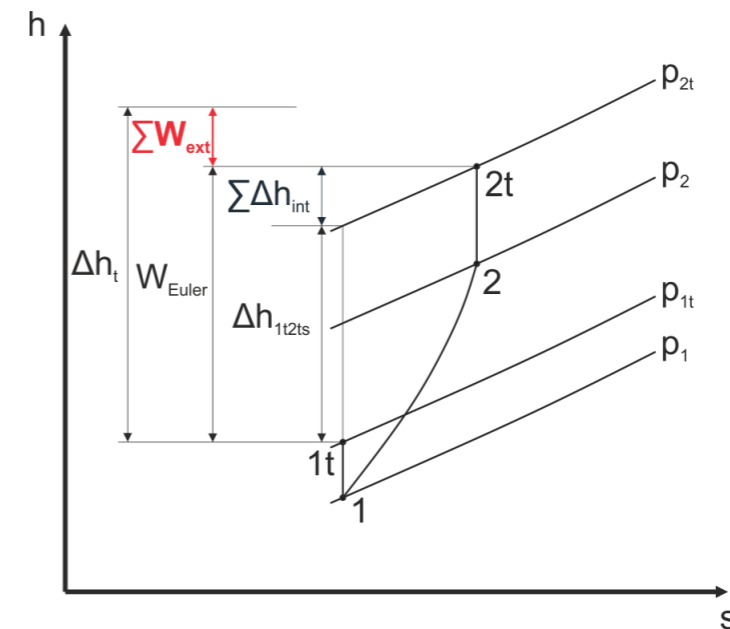




## Meanline Analysis Method

- Single-zone modeling approach
- Implemented in PYTHON with direct calls to the CoolProp [10] property library
- Applied loss model set is based on an optimised and validated set of internal and external loss for conventional centrifugal compressors (Oh et al. [11])

Loss mechanism	Loss model	Reference
<b>External</b>		
Disk Friction	$W_{df} = f_{df} \frac{\bar{\rho} r_2^2 u_2^3}{4\dot{m}}$	Daily and Nece [16] as quoted by Oh et al. [11]
Recirculation	$W_{rc} = 8 \cdot 10^{-5} \sinh(3.5\alpha_2^3) D_f^2 u_2^2$	Oh et al. [11]
Leakage	$W_{lk} = \frac{\dot{m}_{cl} u_{cl} u_2}{2\dot{m}}$	Aungier [17]

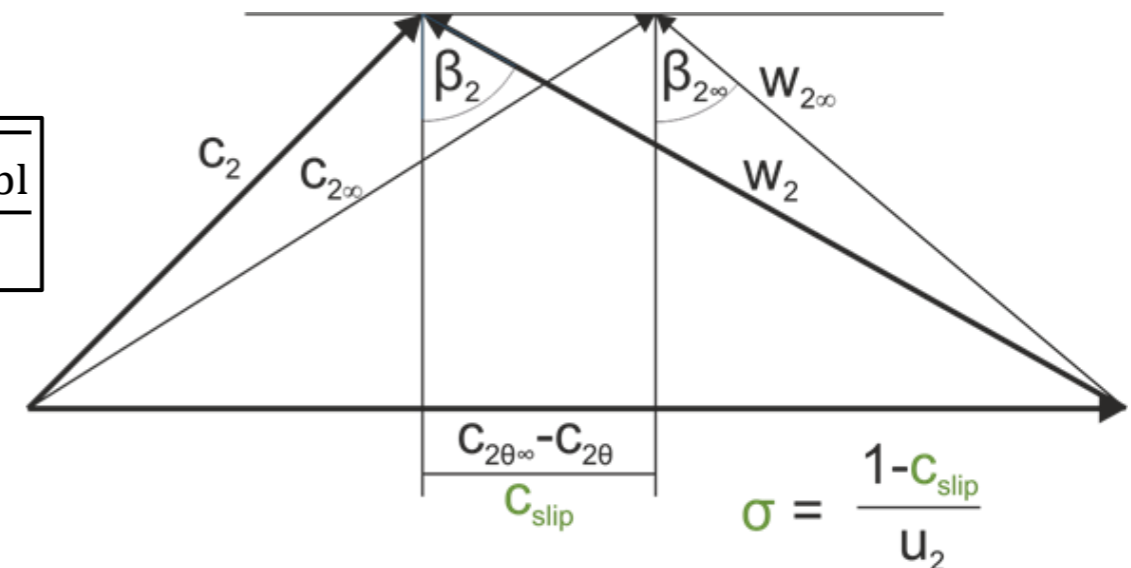


## Meanline Analysis Method

- Single-zone modeling approach
- Implemented in PYTHON with direct calls to the CoolProp [10] property library
- Applied loss model set is based on an optimised and validated set of internal and external loss for conventional centrifugal compressors (Oh et al. [11])
- Wiesner slip correlation [18]

Loss mechanism	Loss model	Reference
<b>External</b>		
Disk Friction	$W_{df} = f_{df} \frac{\bar{\rho} r_2^2 u_2^3}{4\dot{m}}$	Daily and Nece [16] as quoted by Oh et al. [11]
Recirculation	$W_{rc} = 8 \cdot 10^{-5} \sinh(3.5\alpha_2^3) D_f^2 u_2^2$	Oh et al. [11]
Leakage	$W_{lk} = \frac{\dot{m}_{cl} u_{cl} u_2}{2\dot{m}}$	Aungier [17]

$$\sigma = 1 - \frac{\sqrt{\cos \beta_{2,bl}}}{Z_{bl}^2}$$



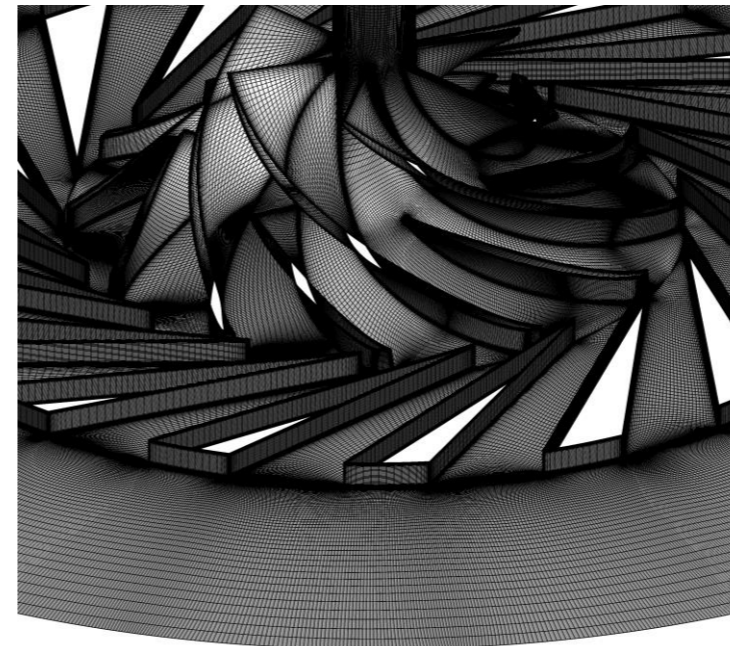
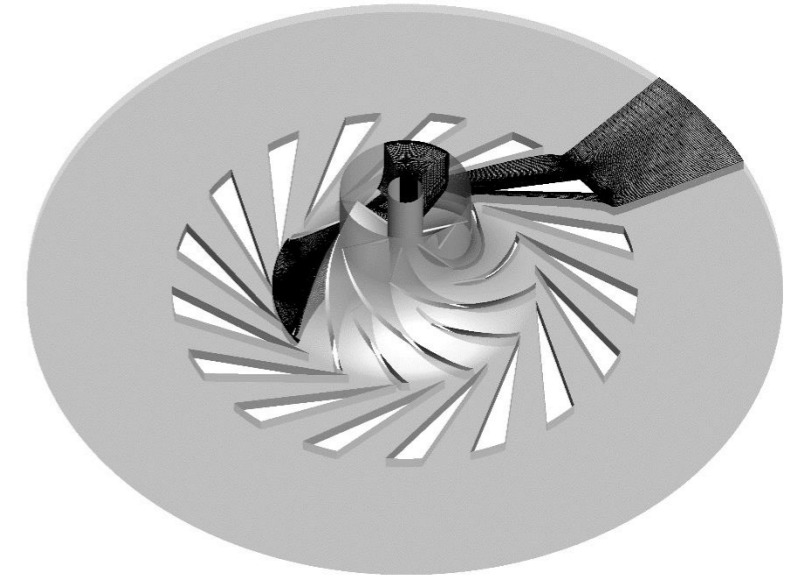
## Meanline Analysis Method

- Single-zone modeling approach
- Implemented in PYTHON with direct calls to the CoolProp [10] property library
- Applied loss model set is based on an optimised and validated set of internal and external loss for conventional centrifugal compressors (Oh et al. [11])
- Wiesner slip correlation [18]
- Diffuser model adopted from Aungier [19]

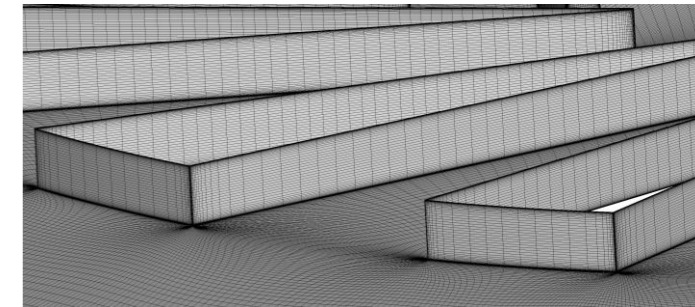
Loss mechanism	Loss model	Reference
<b>Diffuser</b>		
Incidence	$\bar{\omega}_{inc} = \begin{cases} 0.8[(c_3 - c_3^*)/c_3]^2 & c_3 \leq c_{3S} \\ 0.8[((c_3/c_{3S})^2 - 1) c_{th}^2/c_3^2 + (c_{3S} - c_3^*)^2/c_{3S}^2] & c_3 > c_{3S} \end{cases}$	Aungier [19]
Skin friction	$\bar{\omega}_{sf} = 4c_{f,diff}(\bar{c}/c_3)^2 L_B/d_{h,diff}/(2\delta/d_{h,diff})^{0.25}$	Aungier [19]
Mixing	$\bar{\omega}_{mix} = [(c_{m,wake} - c_{m,mix})/c_3]^2$	Aungier [19]

## CFD Analysis - Numerical Setup

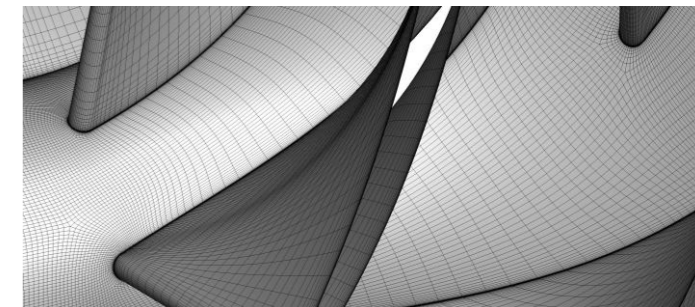
- Steady state RANS simulations
  - Second order AUSM+ scheme [20]
  - Implicit LUSGS scheme
- Spalart-Allmaras turbulence model [21]
- Homogenous equilibrium mixture (HEM)
- Block structured mesh
  - No wall functions:  $y^+ < 5$
  - $\approx 1.5$  mio. cells for single main + splitter blade
  - $\approx 630k$  cells for single diffuser passage
- Mixing-Plane RS-Interface



Replicated surface mesh



Diffuser trailing edge

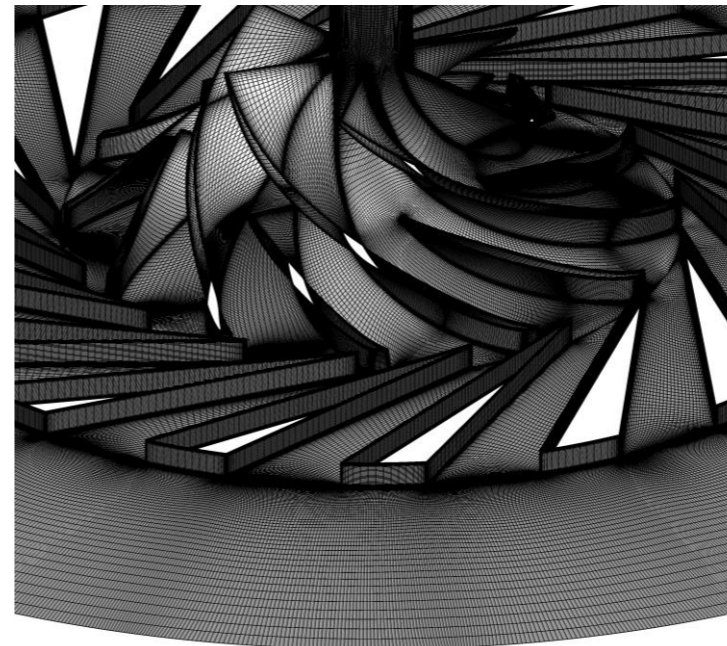
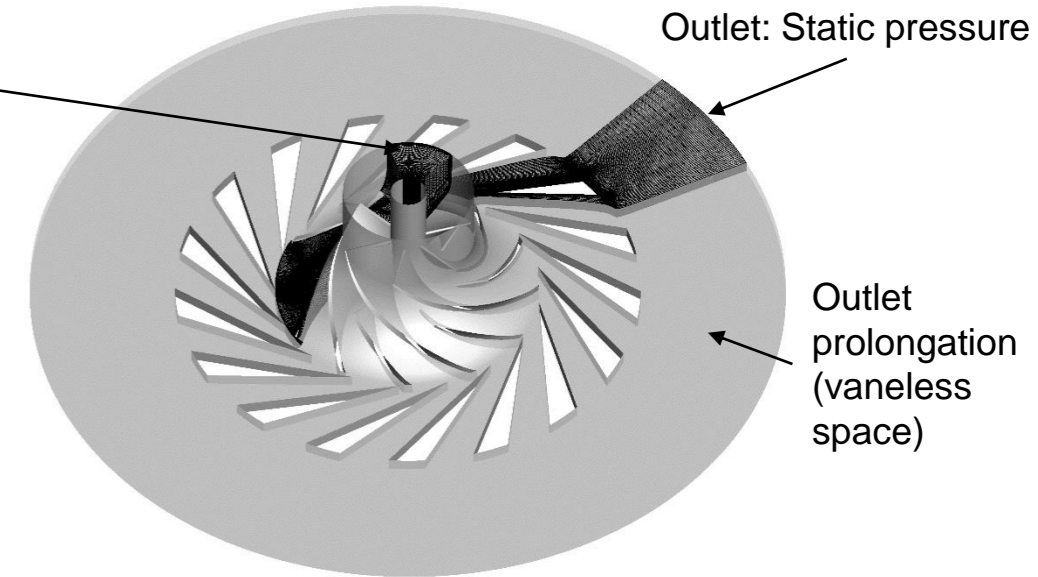


Impeller blade passage

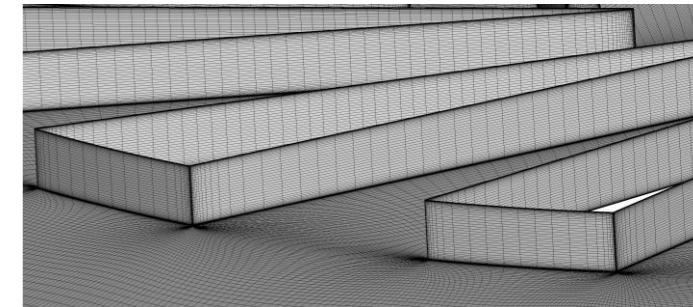
## CFD Analysis - Numerical Setup

- Steady state RANS simulations
  - Second order AUSM+ scheme [20]
  - Implicit LUSGS scheme
- Spalart-Allmaras turbulence model [21]
- Homogenous equilibrium mixture (HEM)
- Block structured mesh
  - No wall functions:  $y^+ < 5$
  - $\approx 1.5$  mio. cells for single main + splitter blade
  - $\approx 630k$  cells for single diffuser passage
- Mixing-Plane RS-Interface

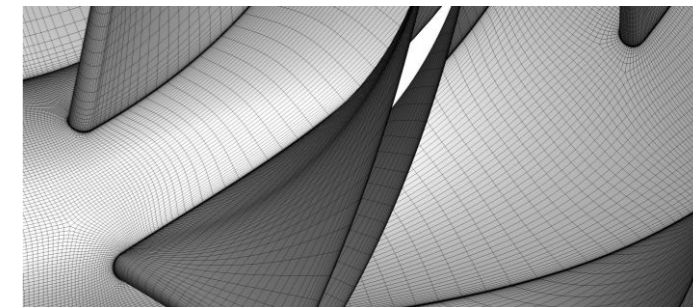
Inlet:  
- Total temperature  
- Total pressure  
- Uniform and normal flow



Replicated surface mesh



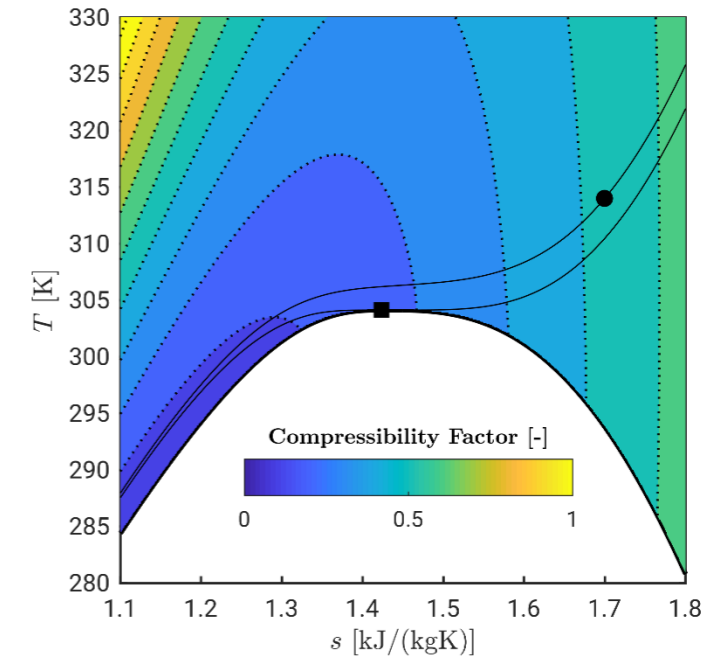
Diffuser trailing edge



Impeller blade passage

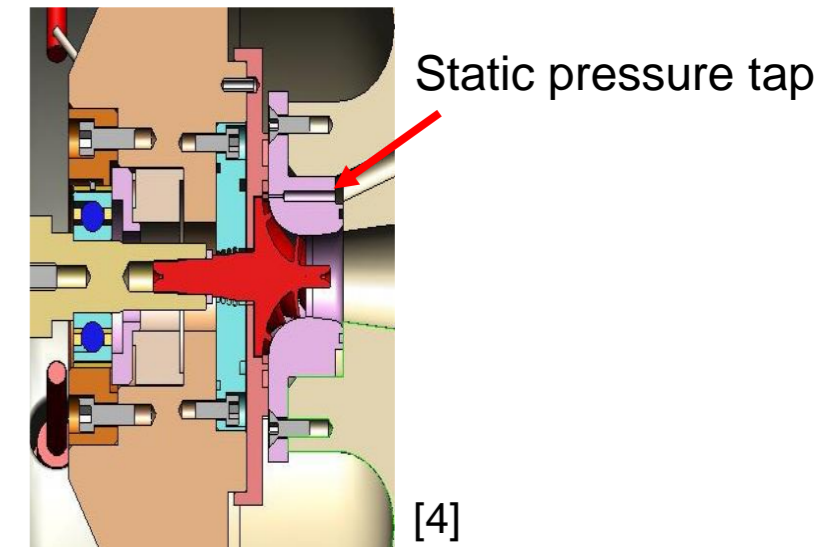
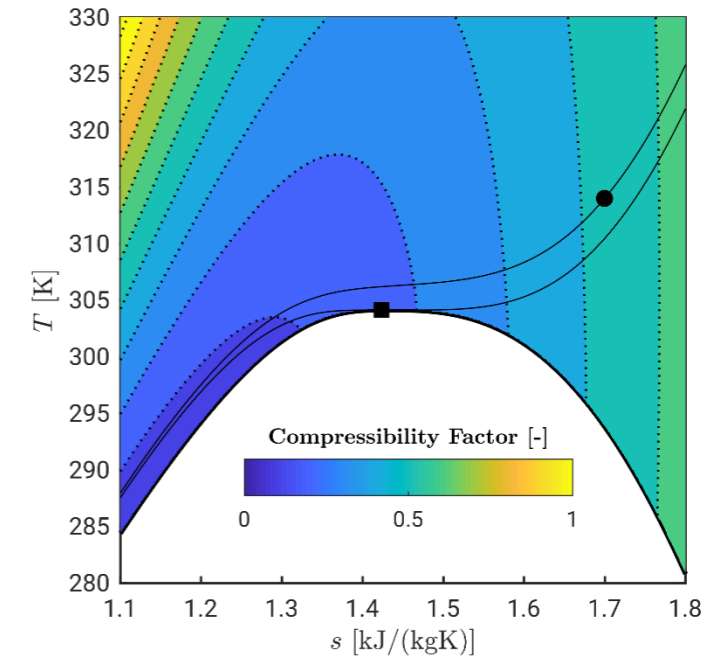
## Investigated Compressor Operating Condition

- Inlet state:  
77.5 bar ( $p/p_c \approx 1.04$ ), 314 K ( $T/T_c \approx 1.03$ ),  $Z \approx 0.53$
- 50 krpm speedline calculation (off-design)  
→ most data available
- Comparison with experimental data of Wright et al. [4, 22] and Fuller & Eisemann [23] and previous numerical study (Karaefe et al. [9]) considering the impeller geometry



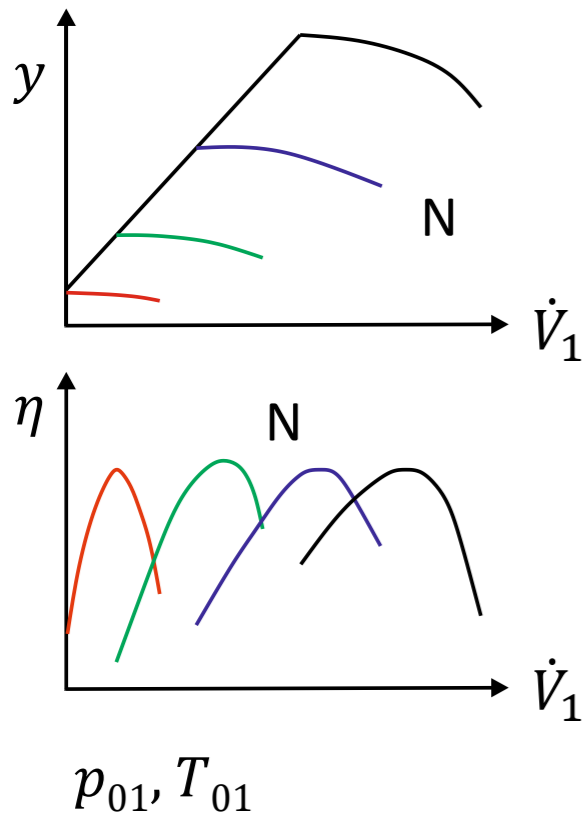
## Investigated Compressor Operating Condition

- Inlet state:  
77.5 bar ( $p/p_c \approx 1.04$ ), 314 K ( $T/T_c \approx 1.03$ ),  $Z \approx 0.53$
- 50 krpm speedline calculation (off-design)  
→ most data available
- Comparison with experimental data of Wright et al. [4, 22] and Fuller & Eisemann [23] and previous numerical study (Karaefe et al. [9]) considering the impeller geometry
- Experimental performance assessments (total-to-static) are interpreted to be associated with the impeller wheel (static pressure tap at impeller exit)
- Strong variation of experimental inlet states  
→ corrected and non-dimensional performance map representation

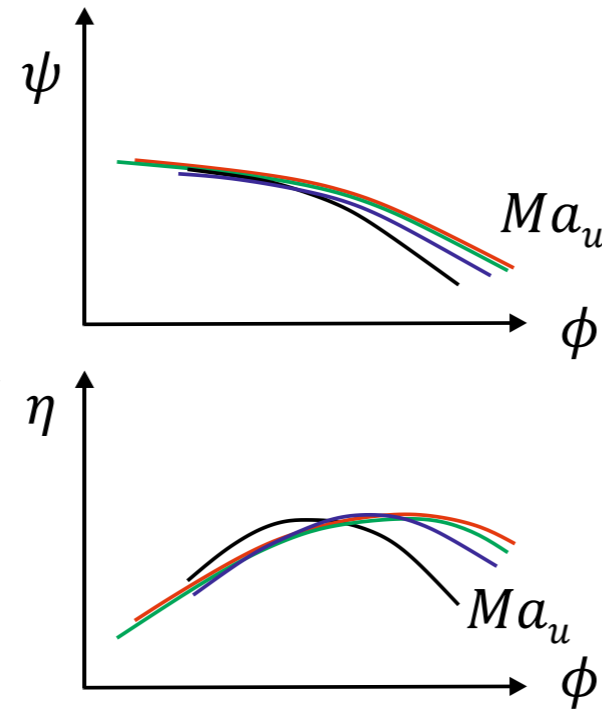


## Performance Assessment

dimensional



non-dimensional



$$\phi = \frac{4\dot{V}_1}{\pi d_2^2 u_2}$$

Flow Coefficient

$$\psi_{12} = \frac{h_{2s} - h_{01}}{u_2^2}$$

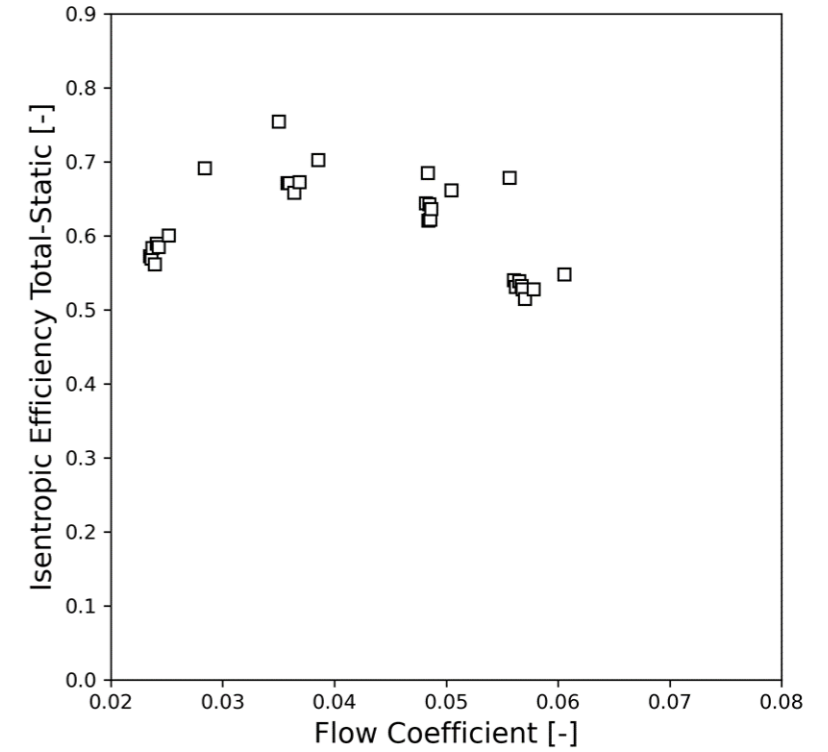
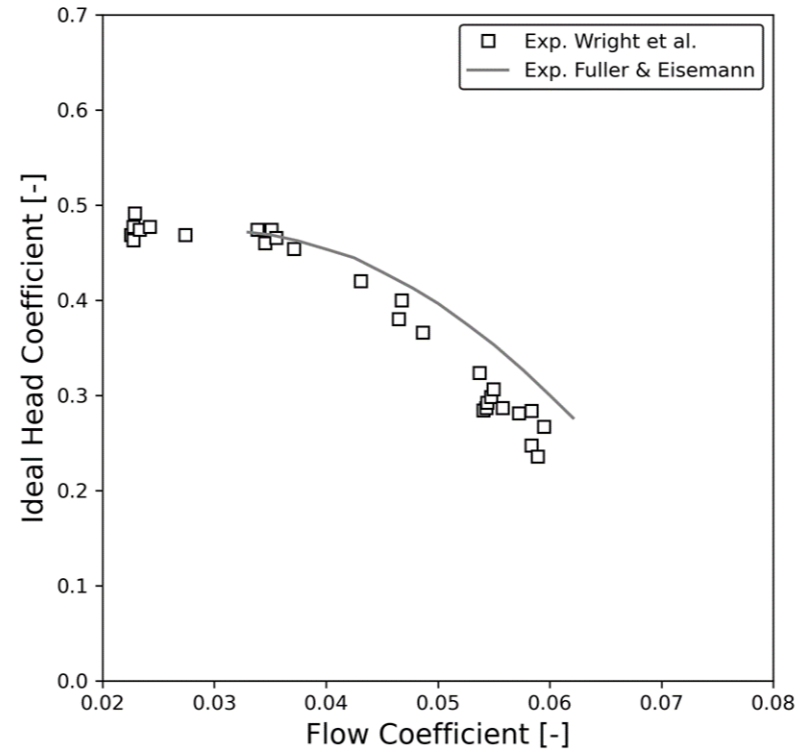
Ideal Head Coefficient

$$\eta_{s,12} = \frac{h_{2s} - h_{01}}{h_{02} - h_{01}}$$

Isentropic Efficiency

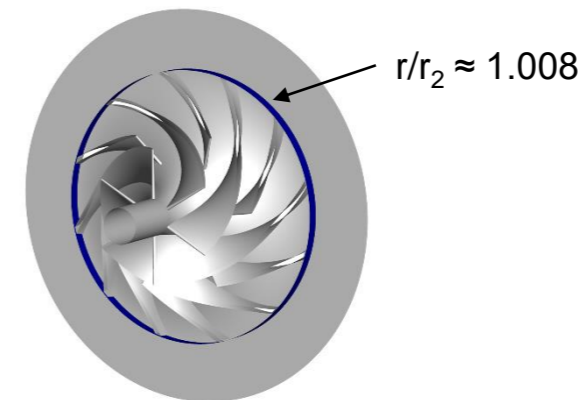
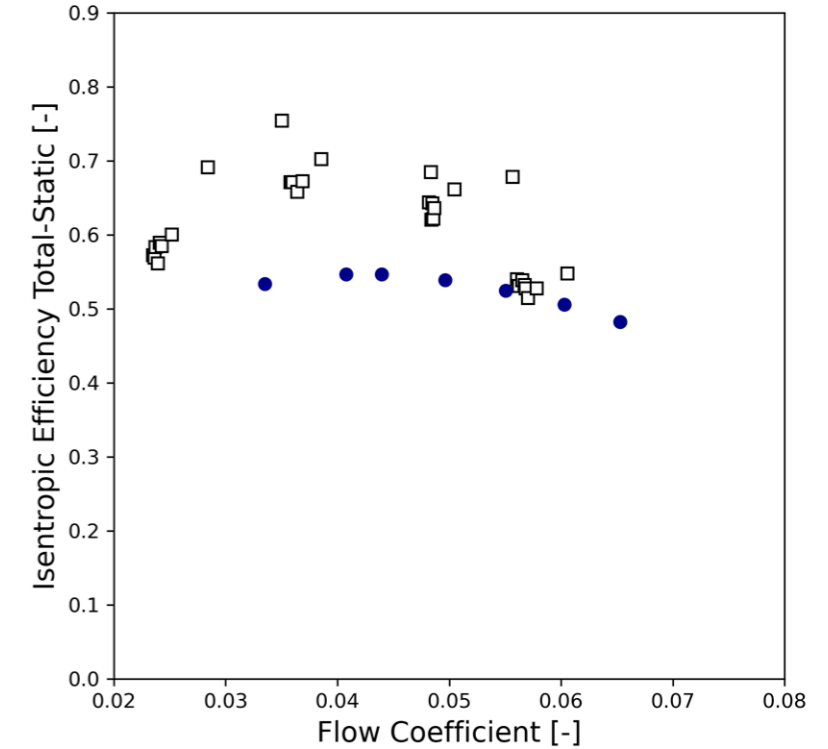
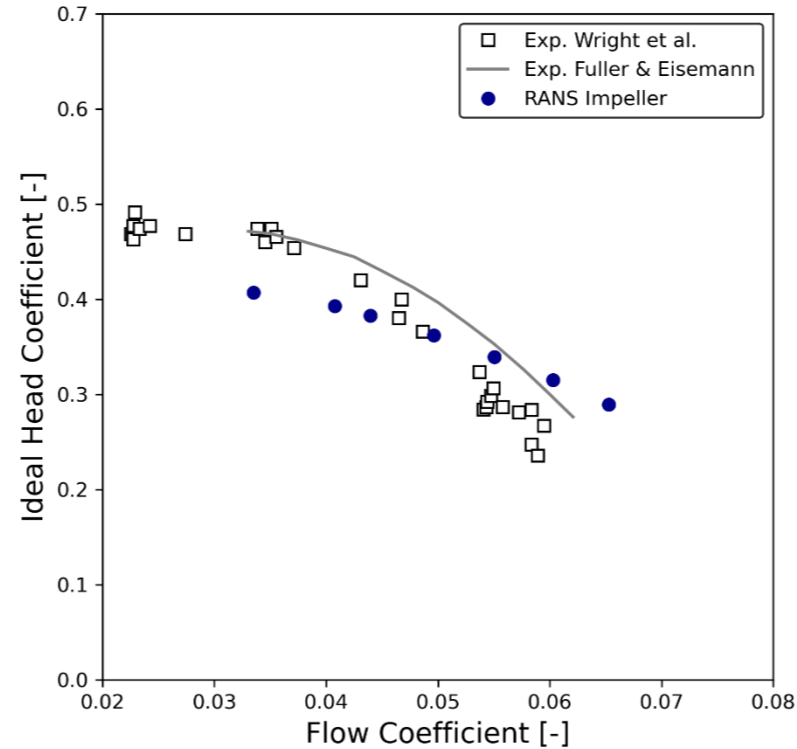


## Non-Dimensional Performance



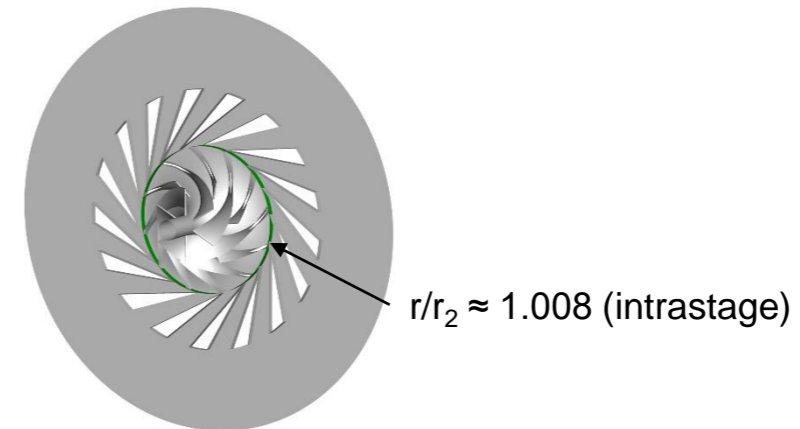
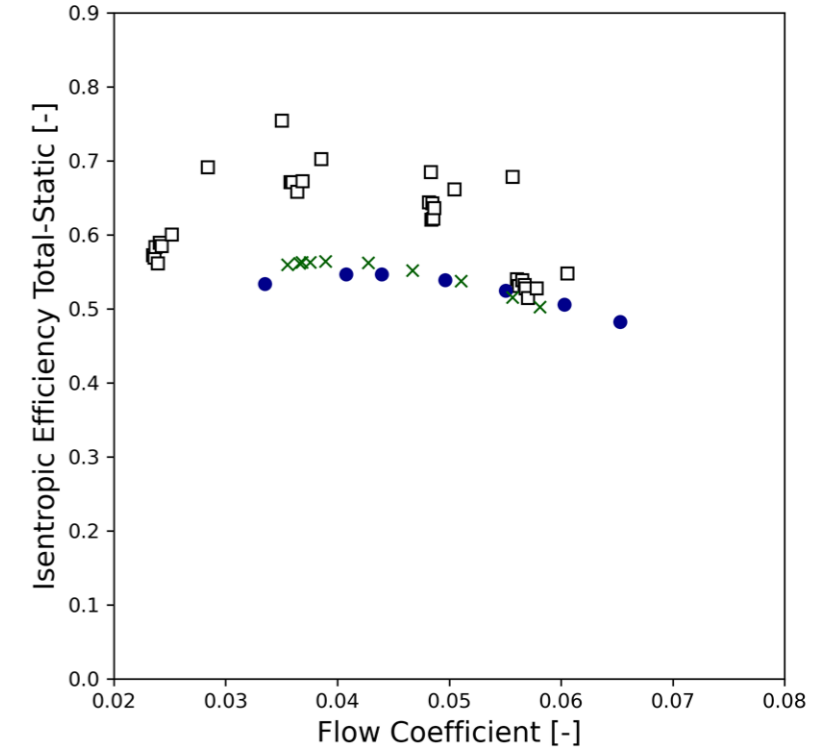
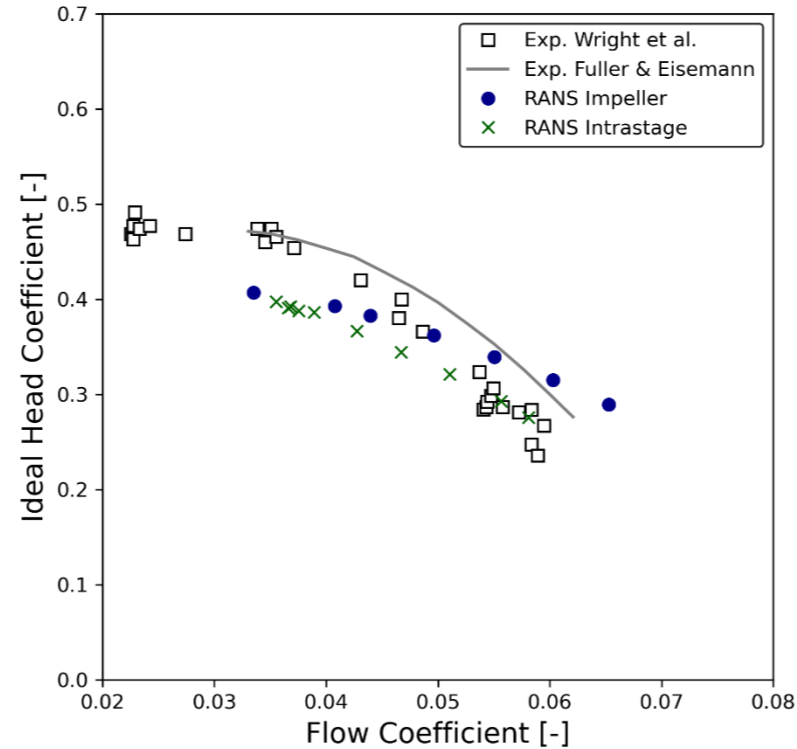
## Non-Dimensional Performance

- RANS - Impeller only [9]
  - Flatter head characteristic
  - Reduced efficiencies
  - Surge comparable
  - Flow coefficient for max. efficiency comparable



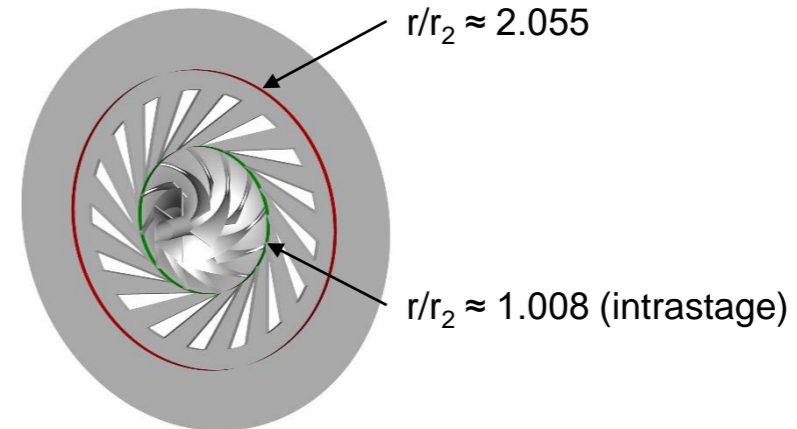
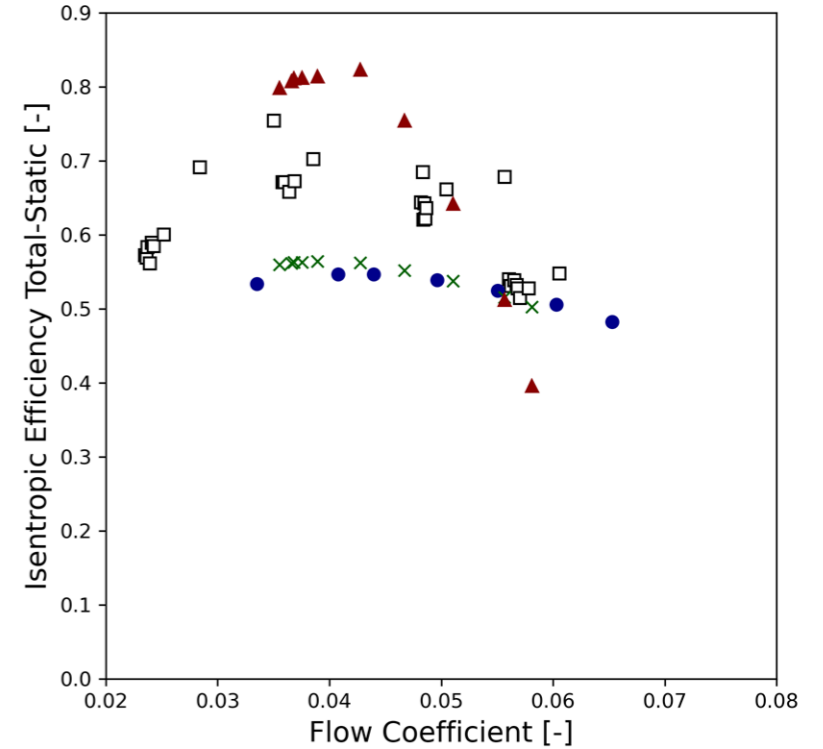
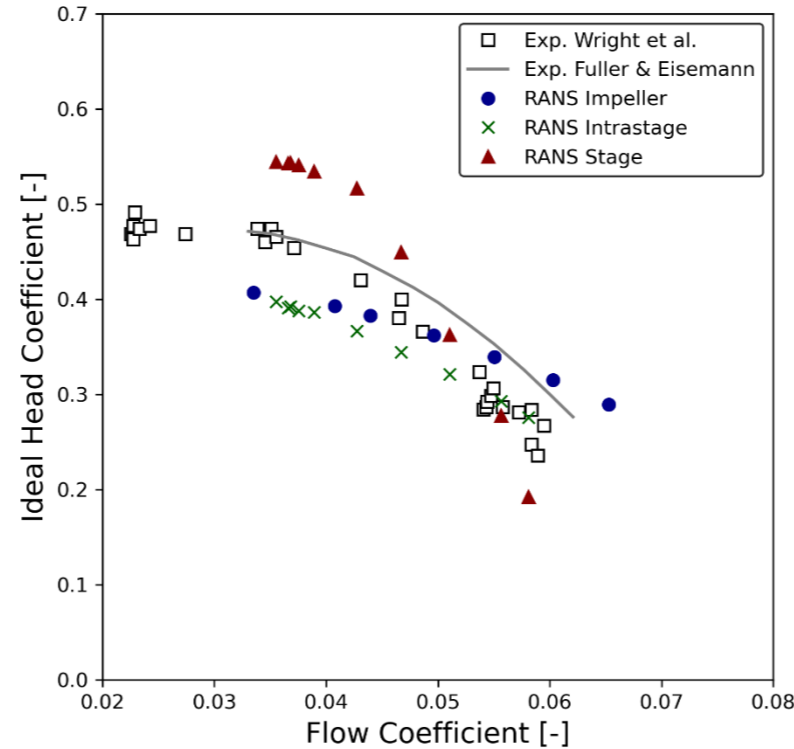
## Non-Dimensional Performance

- RANS - Impeller performance assessment at intrastage position
  - Steeper head characteristic compared to previous setup
  - Comparable efficiencies between both setups



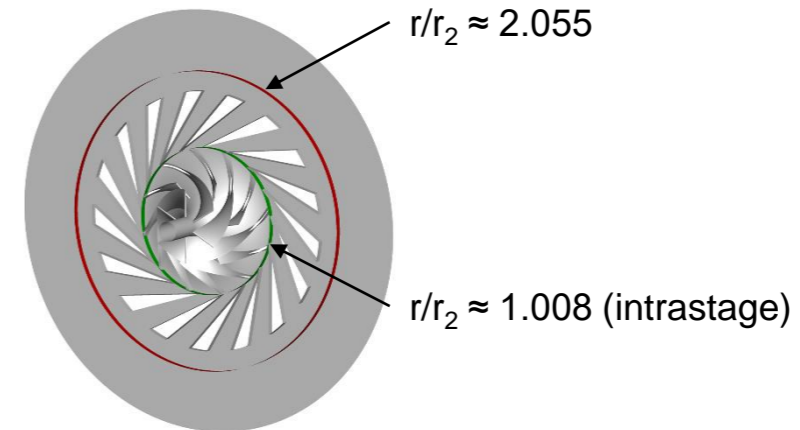
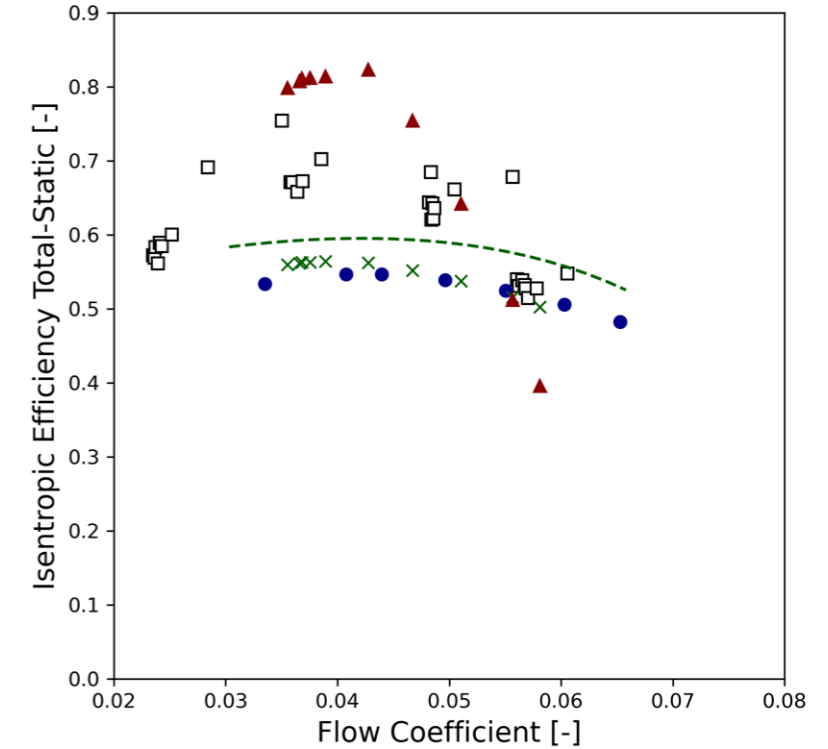
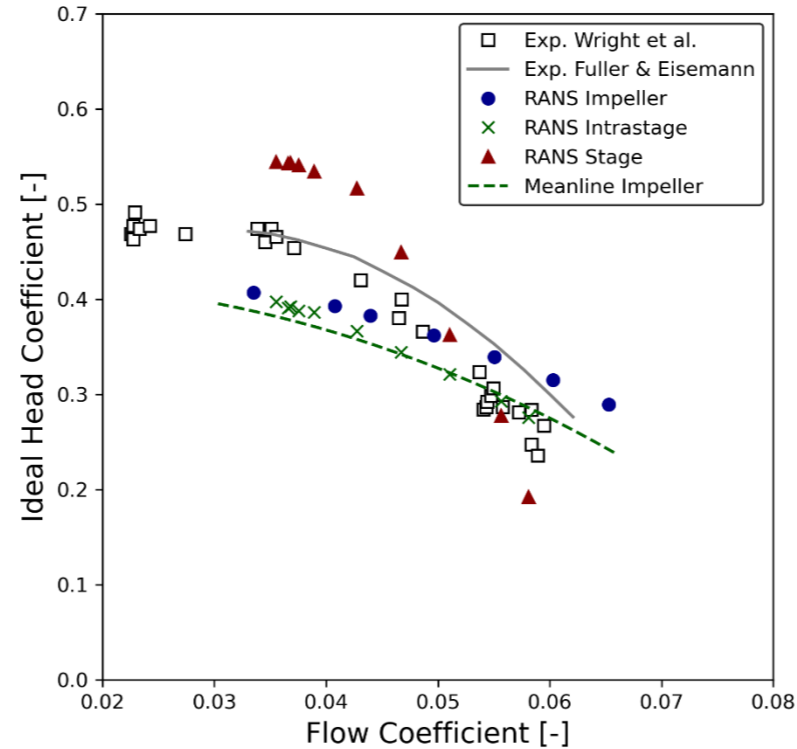
## Non-Dimensional Performance

- RANS - Impeller performance assessment at intrastage position
  - Steeper head characteristic compared to previous setup
  - Comparable efficiencies between both setups
- RANS - Stage performance assessment
  - Ideal head rise of 13-41% for  $\phi \approx 0.036 \dots 0.051$
  - Maximum efficiency  $\approx 82\%$  (t-s)
  - Steep decline in head and efficiency for  $\phi > 0.043$



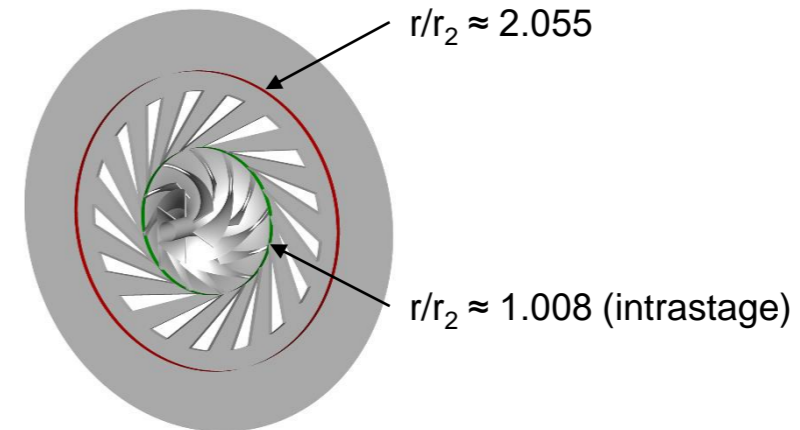
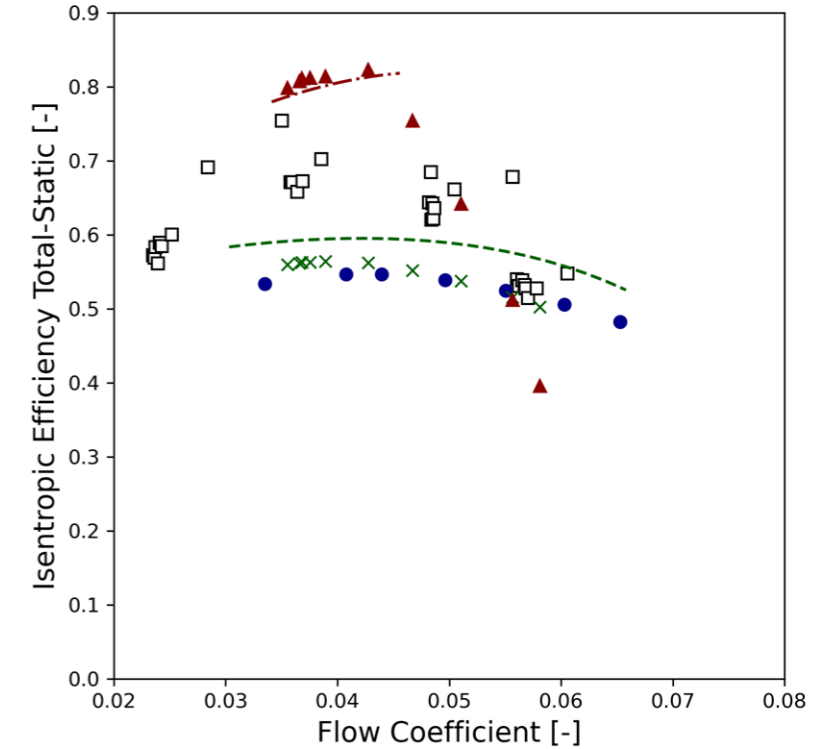
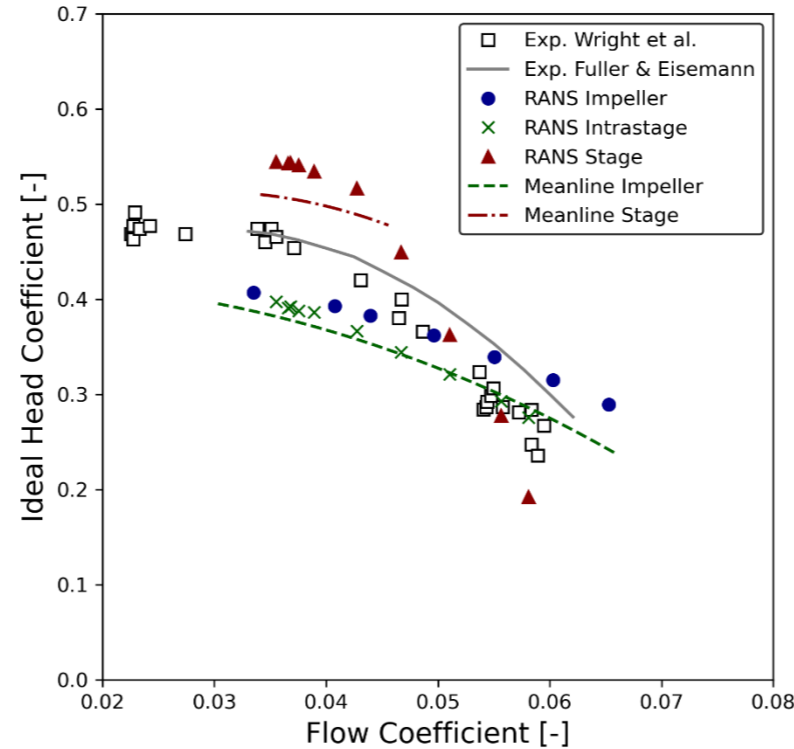
## Non-Dimensional Performance

- Meanline impeller assessment
  - Ideal head curve shows better agreement with the intrastage impeller assessment
  - Maximum impeller efficiency  $\approx 60\%$  (t-s)



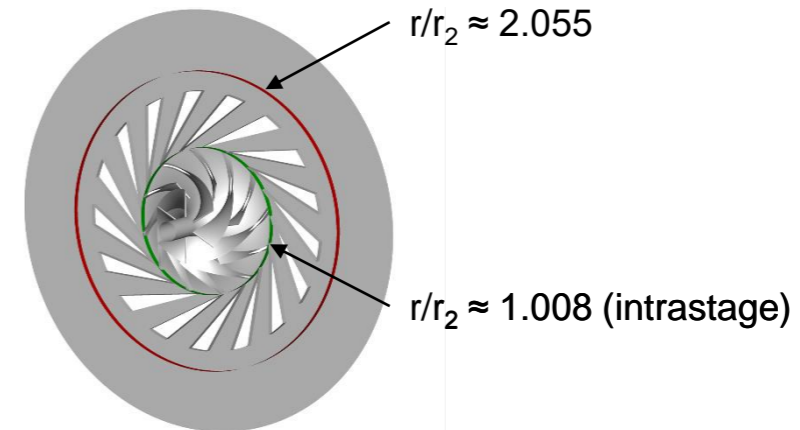
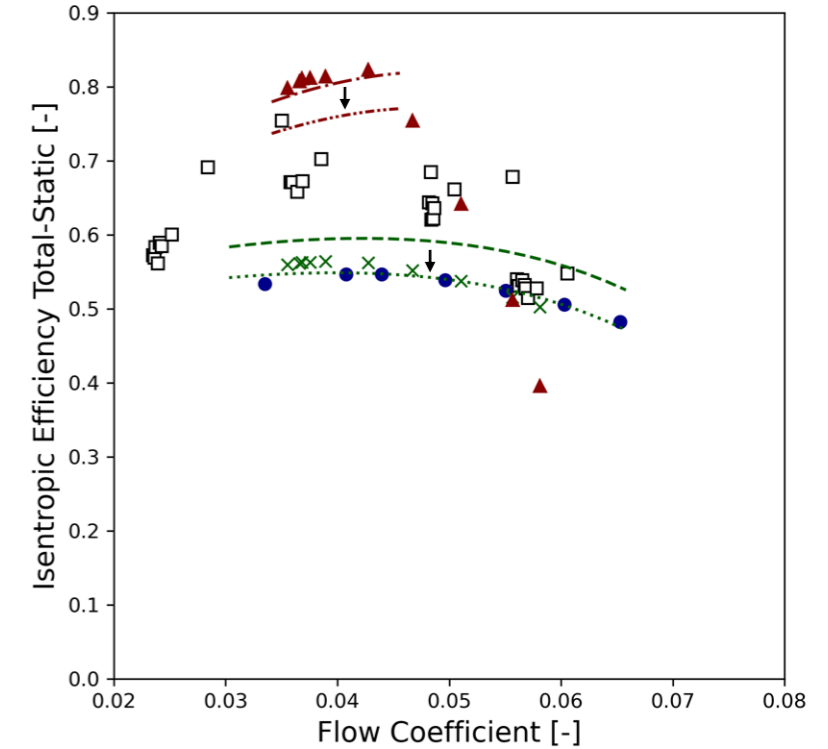
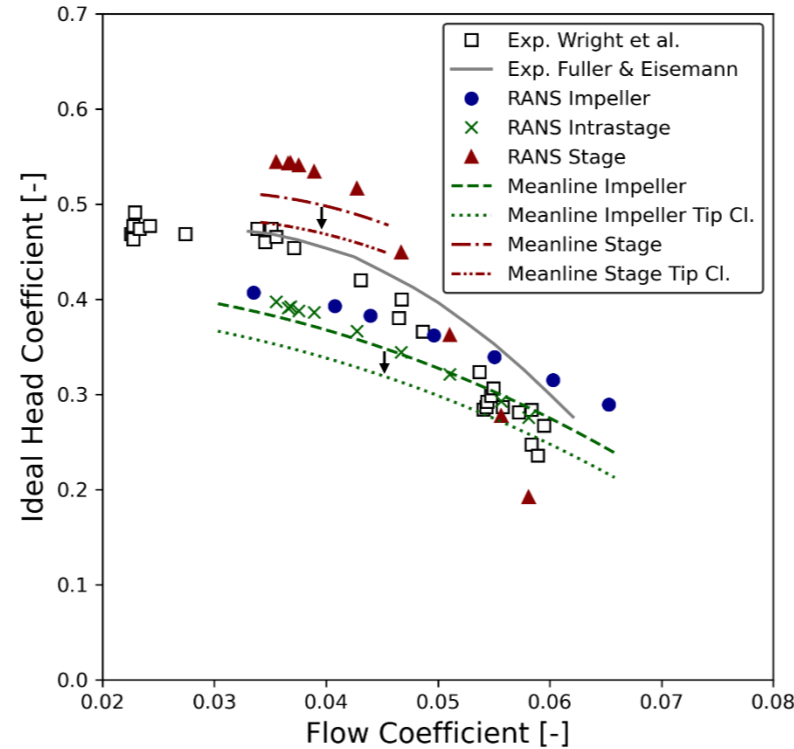
## Non-Dimensional Performance

- Meanline impeller assessment
  - Ideal head curve shows better agreement with the intrastage impeller assessment
  - Maximum impeller efficiency  $\approx 60\%$  (t-s)
- Meanline stage assessment
  - 6-7% reduced ideal head compared to RANS calculations for flow coefficients up to  $\phi \approx 0.043$
  - Abrupt decline in ideal head and efficiency can not be resembled by the diffuser model



## Non-Dimensional Performance

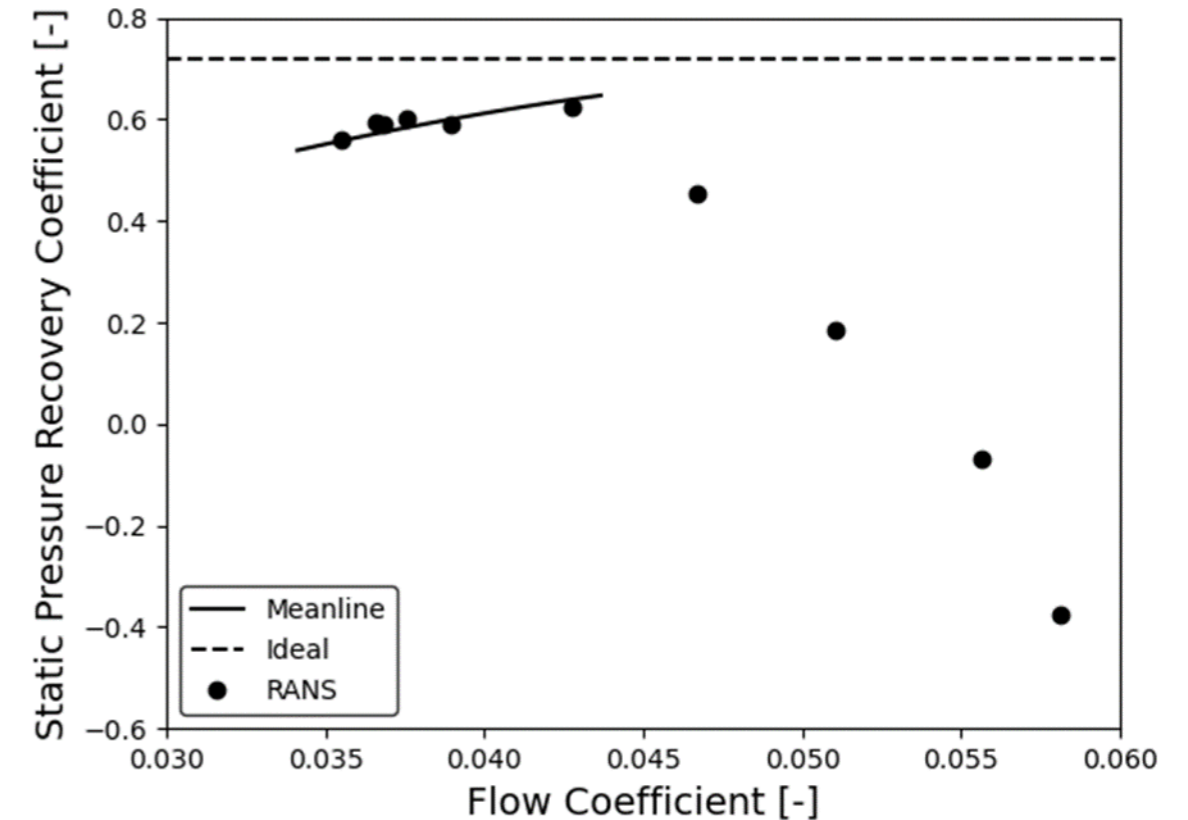
- Consideration of impeller tip clearance in meanline assessment:
  - 7-11% decrease in impeller head generation
  - 4-5 percentage points decrease in impeller efficiency



## Diffuser performance

- Efficient pressure recovery in the range  $\phi \approx 0.036 \dots 0.043$
- Good agreement between meanline and RANS prediction for the flow range with efficient recovery

$$C_p = \frac{p_{out} - p_{in}}{p_{0,in} - p_{in}} \quad \text{Static Pressure Recovery Coefficient}$$

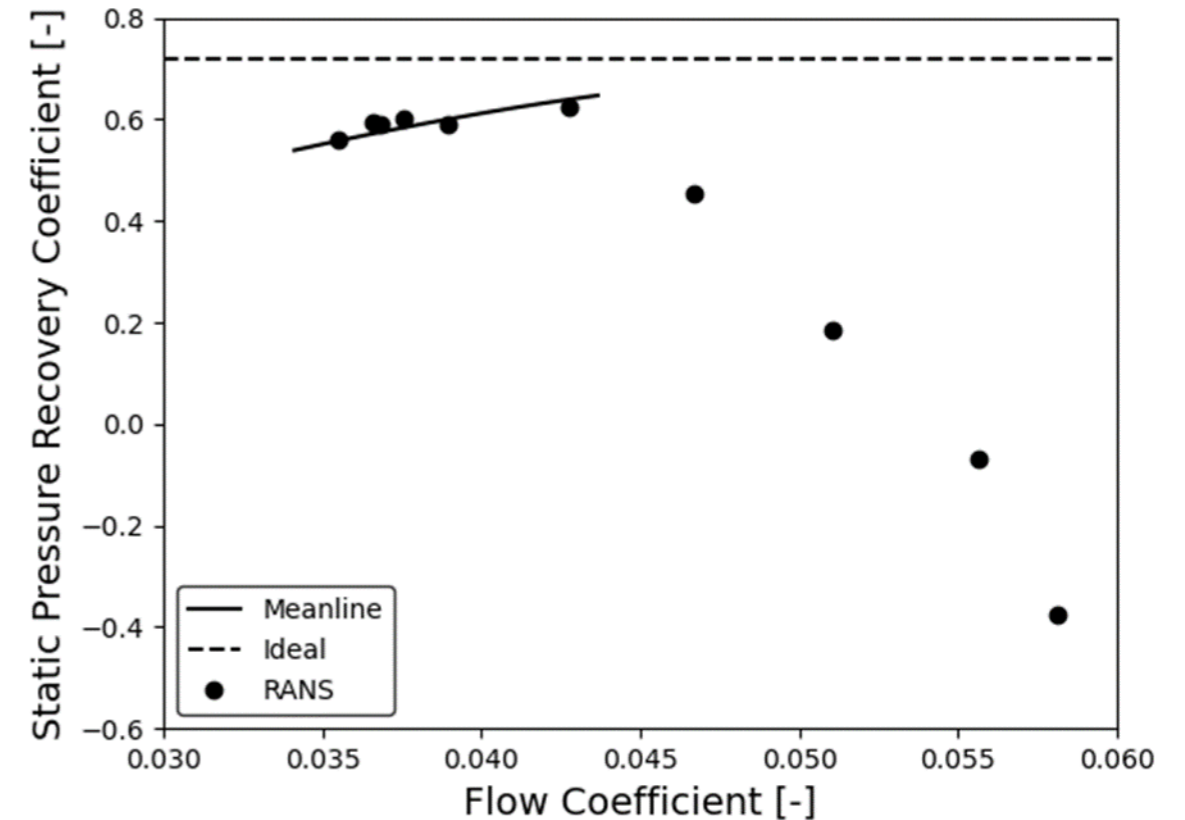




## Diffuser performance

- Efficient pressure recovery in the range  $\phi \approx 0.036 \dots 0.043$
- Good agreement between meanline and RANS prediction for the flow range with efficient recovery
- RANS:
  - Continuous decline in  $c_p$  for  $\phi > 0.043$
  - Negative  $c_p$  for  $\phi > 0.051$   
( $p_{0,out} < p_{in}$ )

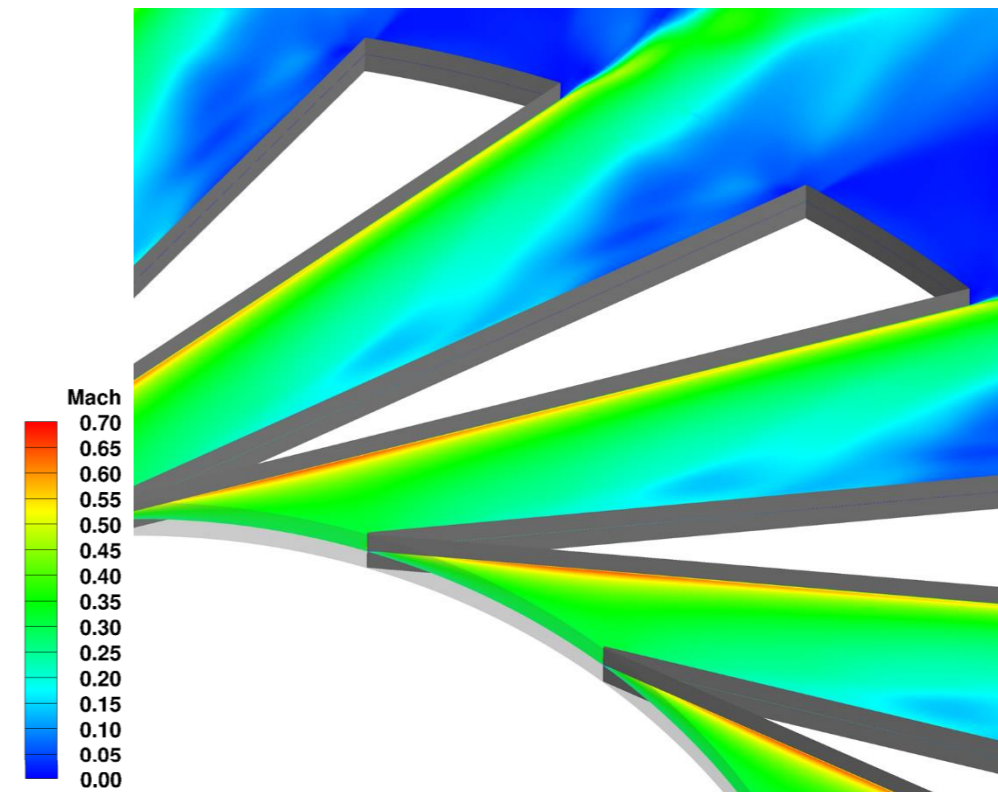
$$c_p = \frac{p_{out} - p_{in}}{p_{0,in} - p_{in}} \quad \text{Static Pressure Recovery Coefficient}$$



## Diffuser performance

- Efficient pressure recovery in the range  $\phi \approx 0.036 \dots 0.043$
- Good agreement between meanline and RANS prediction for the flow range with efficient recovery
- RANS:
  - Continuous decline in  $c_p$  for  $\phi > 0.043$
  - Negative  $c_p$  for  $\phi > 0.051$  ( $p_{0,out} < p_{in}$ )
  - Flow separation in channel diffuser passage

$$c_p = \frac{p_{out} - p_{in}}{p_{0,in} - p_{in}} \quad \text{Static Pressure Recovery Coefficient}$$



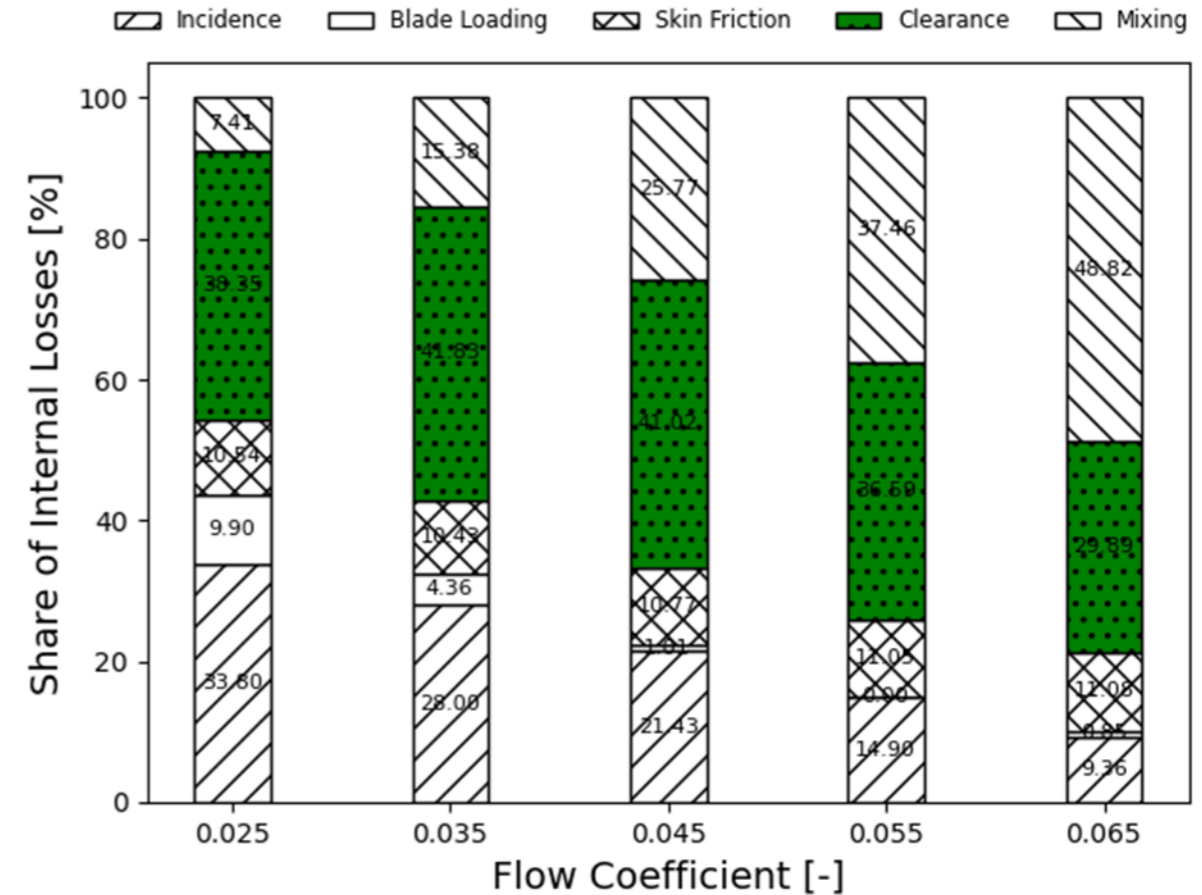
Contours of Mach number  
at 50 % span for  $\phi \approx 0.058$

## Meanline Loss Distribution

- Clearance loss with significant share over the entire flow range ( $\approx 30\text{-}42\%$ )

$$\text{SNL: } \frac{\delta}{d_2} \approx 0.007$$

$$\text{Eckardt Impeller: } \frac{\delta}{d_2} \approx 0.001$$



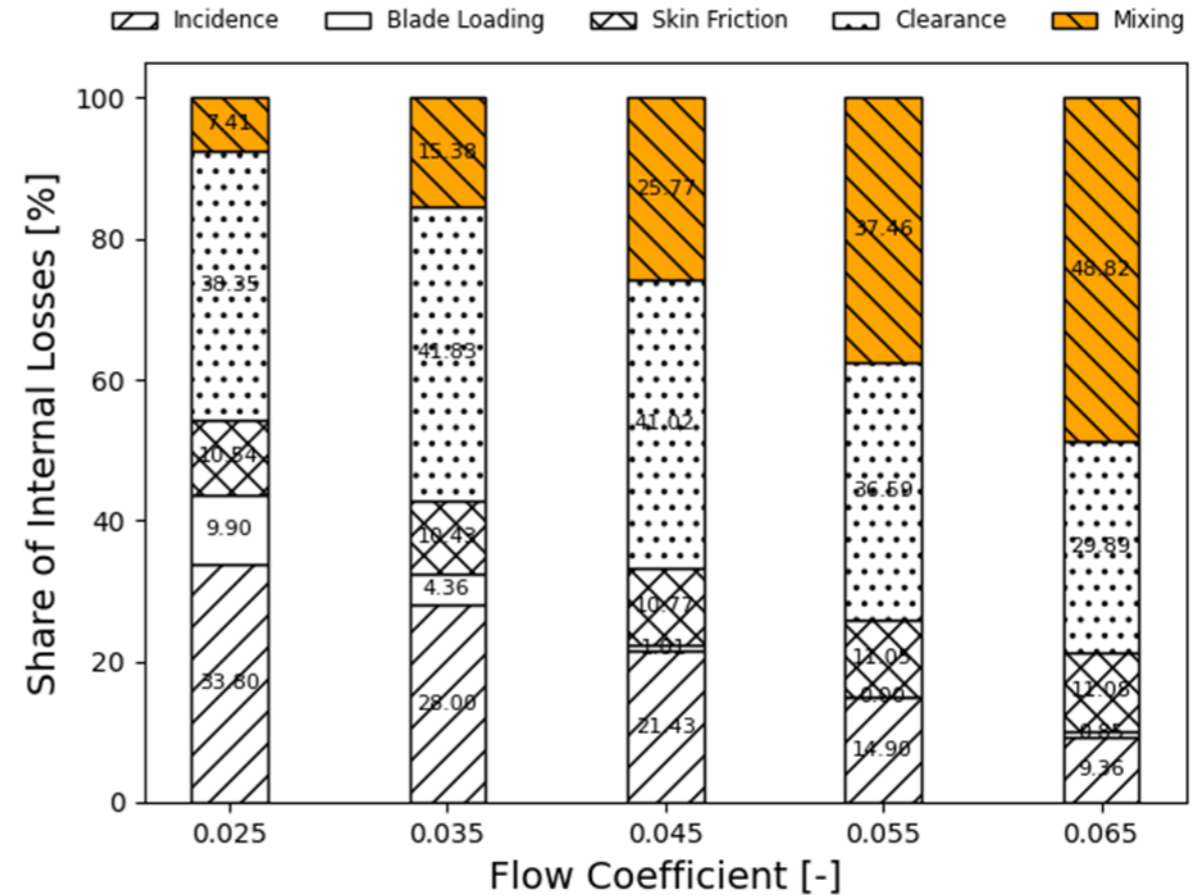
## Meanline Loss Distribution

- Clearance loss with significant share over the entire flow range ( $\approx 30\text{-}42\%$ )

$$\text{SNL: } \frac{\delta}{d_2} \approx 0.007$$

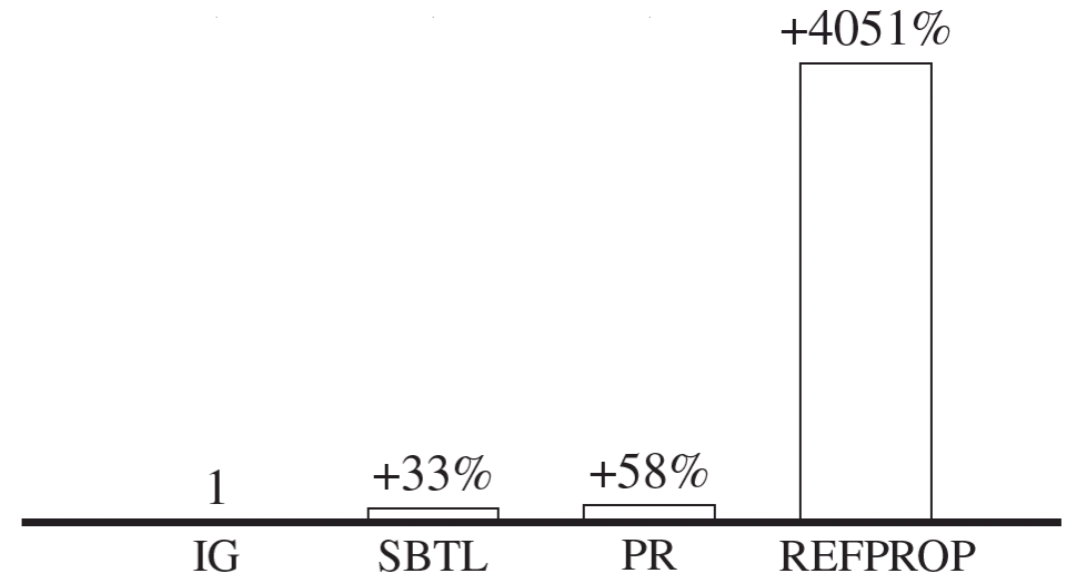
$$\text{Eckardt Impeller: } \frac{\delta}{d_2} \approx 0.001$$

- Wake mixing losses dominant in meanline prediction at high flow coefficients



## Benchmark

- IG and PR simulations performed without tabulation
- Direct calls to REFPROP library
- Further reduction of overhead might be expected in future versions of the SBTL library (2% overhead demonstrated for the highly optimised steam version)



## Conclusion

## Conclusion

- Reasonable performance metrics derived despite approximations of the candidate compressor geometry

## Conclusion

- Reasonable performance metrics derived despite approximations of the candidate compressor geometry
- Meanline analysis satisfyingly resembles the CFD impeller performance and the CFD stage characteristics in the flow coefficient range with practical ideal head recovery



## Conclusion

- Reasonable performance metrics derived despite approximations of the candidate compressor geometry
- Meanline analysis satisfyingly resembles the CFD impeller performance and the CFD stage characteristics in the flow coefficient range with practical ideal head recovery
- Meanline loss distributions indicate impeller tip clearance as a dominant loss contributing factor over the entire operating range

## Conclusion

- Reasonable performance metrics derived despite approximations of the candidate compressor geometry
- Meanline analysis satisfyingly resembles the CFD impeller performance and the CFD stage characteristics in the flow coefficient range with practical ideal head recovery
- Meanline loss distributions indicate impeller tip clearance as a dominant loss contributing factor over the entire operating range
- CFD framework comprising the SBTL library allows for accurate calculations within the range of uncertainties of the EOS at comparatively low computational overhead (33% compared to IG)

## Conclusion

- Reasonable performance metrics derived despite approximations of the candidate compressor geometry
- Meanline analysis satisfyingly resembles the CFD impeller performance and the CFD stage characteristics in the flow coefficient range with practical ideal head recovery
- Meanline loss distributions indicate impeller tip clearance as a dominant loss contributing factor over the entire operating range
- CFD framework comprising the SBTL library allows for accurate calculations within the range of uncertainties of the EOS at comparatively low computational overhead (33% compared to IG)

## Consecutive Work

## Conclusion

- Reasonable performance metrics derived despite approximations of the candidate compressor geometry
- Meanline analysis satisfyingly resembles the CFD impeller performance and the CFD stage characteristics in the flow coefficient range with practical ideal head recovery
- Meanline loss distributions indicate impeller tip clearance as a dominant loss contributing factor over the entire operating range
- CFD framework comprising the SBTL library allows for accurate calculations within the range of uncertainties of the EOS at comparatively low computational overhead (33% compared to IG)

## Consecutive Work

- Integration of metastable states and assessment of non-equilibrium condensation

## Conclusion

- Reasonable performance metrics derived despite approximations of the candidate compressor geometry
- Meanline analysis satisfyingly resembles the CFD impeller performance and the CFD stage characteristics in the flow coefficient range with practical ideal head recovery
- Meanline loss distributions indicate impeller tip clearance as a dominant loss contributing factor over the entire operating range
- CFD framework comprising the SBTL library allows for accurate calculations within the range of uncertainties of the EOS at comparatively low computational overhead (33% compared to IG)

## Consecutive Work

- Integration of metastable states and assessment of non-equilibrium condensation
- Analysis of the aerodynamic loss distribution through CFD

## Conclusion

- Reasonable performance metrics derived despite approximations of the candidate compressor geometry
- Meanline analysis satisfyingly resembles the CFD impeller performance and the CFD stage characteristics in the flow coefficient range with practical ideal head recovery
- Meanline loss distributions indicate impeller tip clearance as a dominant loss contributing factor over the entire operating range
- CFD framework comprising the SBTL library allows for accurate calculations within the range of uncertainties of the EOS at comparatively low computational overhead (33% compared to IG)

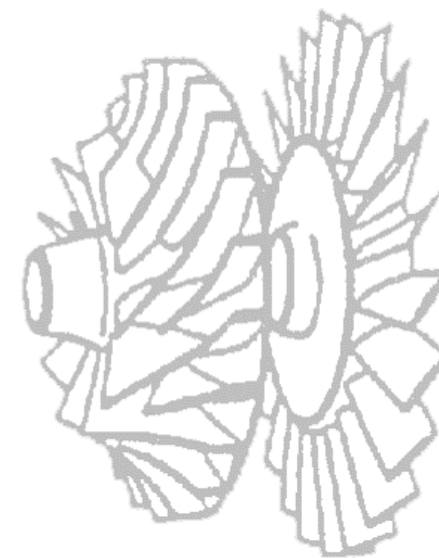
## Consecutive Work

- Integration of metastable states and assessment of non-equilibrium condensation
- Analysis of the aerodynamic loss distribution through CFD
- Transient simulations for improved assessment of rotor-stator interaction

# THANK YOU

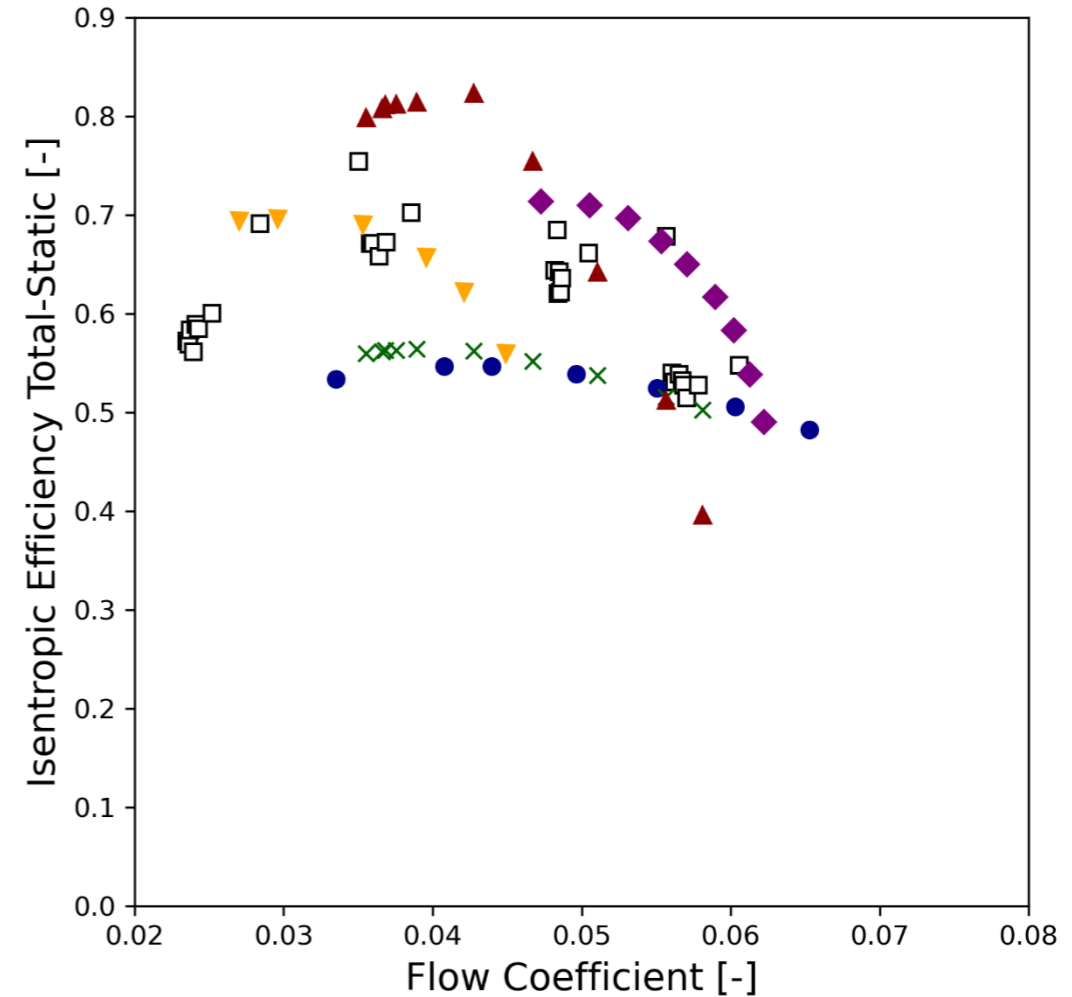
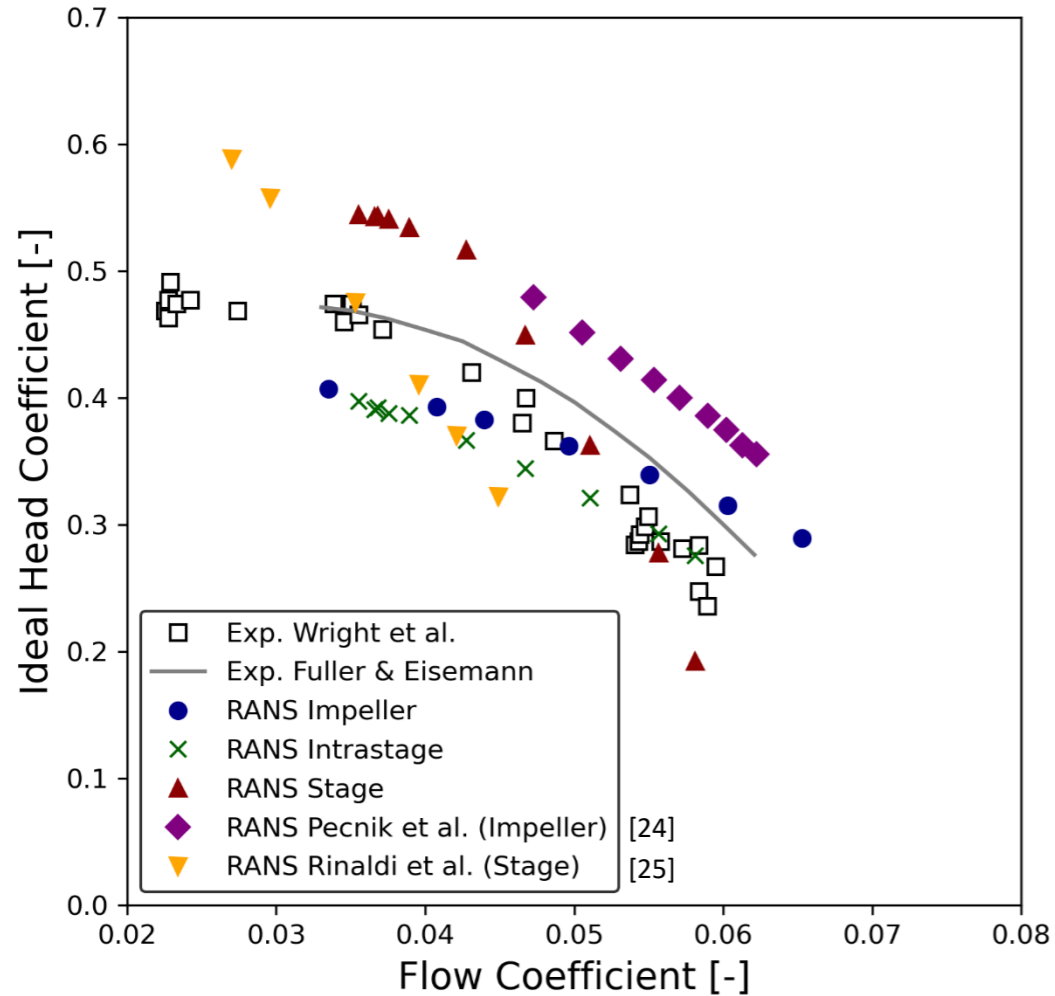
**Renan Emre Karaefe**

[emre.karaefe@rub.de](mailto:emre.karaefe@rub.de)



- [1] R. Span and W. Wagner: "A New Equation of State for Carbon Dioxide Covering the Fluid Region from the Triple-Point Temperature to 1100 K at Pressures up to 800 MPa". J. Phys. Chem. Ref. Data, 25(6), 1996.
- [2] M. Kunick: "Fast Calculation of Thermophysical Properties in Extensive Process Simulations with the Spline-Based Table Look-Up Method (SBTL)". Fortschrittberichte VDI, Nr. 618, Reihe 6, Energietechnik, 2018.
- [3] M. Kunick et al.: "CFD Analysis of Steam Turbines With the IAPWS Standard on the Spline-Based Table Look-Up Method (SBTL) for The Fast Calculation of Real Fluid Properties". Proceedings of the ASME Turbo Expo 2015, Paper No. GT2015-43984, 2015.
- [4] S.A. Wright et al.: "Operation and Analysis of a Supercritical CO<sub>2</sub> Brayton Cycle". SANDIA REPORT SAND2010-0171, Sandia National Laboratories, 2010.
- [5] K. Ziája et al.: "Numerical Investigation of a Partially Loaded Supersonic Orc Turbine Stage". J. Eng. Gas Turbines Power, Paper No. GTP-20-1541, 2020.
- [6] P. Post, B. Winhart, and F. di Mare.: "Large Eddy Simulation of a Condensing Wet Steam Turbine Cascade". J. Eng. Gas Turbines Power, Paper No. GTP-20-1526, 2020.
- [7] A. Laesecke and C.D. Muzny.: "Reference Correlation for the Viscosity of Carbon Dioxide". J. Phys. Chem. Ref. Data, 46(1), 2017.
- [8] L. Huber and E.A. Sykioti.: "Reference Correlation of the Thermal Conductivity of Carbon Dioxide from the Triple Point to 1100 K and up to 200 MPa". J. Phys. Chem. Ref. Data, 45(1), 2016.
- [9] R.E. Karaefe et al.: "Numerical Investigation of a Centrifugal Compressor for Supercritical CO<sub>2</sub> Cycles". Proceedings of the ASME Turbo Expo 2020, Paper No. GT2020-15194, 2020.
- [10] I. Bell et al. "Pure and Pseudo-pure Fluid Thermophysical Property Evaluation and the Open-Source Thermophysical Property Library CoolProp". Ind. Eng. Chem. Res., 53(6), 2014.
- [11] H.W. Oh, E.S. Yoon, and M.K. Chung. "An Optimum Set of Loss Models for Performance Prediction of Centrifugal Compressors". Proceedings of the Institution of Mechanical Engineers, Part A: Journal of Power and Energy, 211(4), 1997.
- [12] O. Conrad, K. Raif, and M. Wessels: "The Calculation of Performance Maps for Centrifugal Compressors With Vane-Island Diffusers". Proceedings of the Twenty-fifth Annual International Gas Turbine Conference and Exhibit and Twentysecond Annual Fluids Engineering Conference, New Orleans, Louisiana, USA, 1979
- [13] J.E. Coppage et al.: "Study of Supersonic Radial Compressors for Refrigeration and Pressurization Systems. WADC TECHNICAL REPORT 55-257, Airesearch Manufacturing Company, 1956
- [14] W. Jansen: "A Method for Calculating the Flow in a Centrifugal Impeller When Entropy Gradients Are Present". Royal Society Conference on Internal Aerodynamics (Turbomachinery). Cambridge, UK, 1967.
- [15] J.P. Johnston, R.C. Dean, Jr.: "Losses in Vaneless Diffusers of Centrifugal Compressors and Pumps: Analysis, Experiment, and Design". J. Eng. Power, 88(1), 1966.
- [16] J.W. Daily and R.E. Nece: "Chamber Dimension Effects on Induced Flow and Frictional Resistance of Enclosed Rotating Disks". J. Basic Engineering, 82(1), 1960.
- [17] R.H. Aungier: "Mean Streamline Aerodynamic Performance Analysis of Centrifugal Compressors". J. Turbomach., 117(3), 1995.
- [18] F.J. Wiesner. "A Review of Slip Factors for Centrifugal Impellers". J. Eng. Gas Turbines Power, 89(4), 1967.
- [19] R.H. Aungier: "Centrifugal Compressors. A Strategy for Aerodynamic Design and Performance Analysis". ASME Press, 2000
- [20] P. Post and F. di Mare. "Highly Efficient Euler-Euler Approach for Condensing Steam Flows in Turbomachines". GPPS Montreal 18. Montreal, Canada, 2018.
- [21] P.R. Spalart and S.R. Allmaras. "A One-Equation Turbulence Model for Aerodynamic Flows". 30th Aerospace Sciences Meeting and Exhibit. Reno, Nevada, USA, 1992
- [22] S.A. Wright et al. "Supercritical CO<sub>2</sub> Compression Loop Operation and Test Results". Supercritical CO<sub>2</sub> Power Cycles Symposium. Troy, New York, USA, 2009.
- [23] R.L. Fuller and K. Eisemann. "Centrifugal Compressor Off-Design Performance for Super-Critical CO<sub>2</sub>". Supercritical CO<sub>2</sub> Power Cycles Symposium. Boulder, Colorado, USA, 2011.





[24] R. Pecnik, E. Rinaldi and Piero Colonna: "Computational Fluid Dynamics of a Radial Compressor Operating With Supercritical CO<sub>2</sub>". J. Eng. Gas Turbines Power, 134(12), 2012

[25] E. Rinaldi, R. Pecnik and Piero Colonna: "Computational Fluid Dynamic Simulation of a Supercritical CO<sub>2</sub> Compressor Performance Map". J. Eng. Gas Turbines Power, 137(7), 2014